

Crosstalk between the lipopolysaccharide and phospholipid pathways during outer membrane biogenesis in *Escherichia coli*

Akintunde Emiola, Steven S. Andrews, Carolin Heller, John George

SI APPENDIX

Contents

MODEL FOR LPS/PHOSPHOLIPIDS BIOSYNTHESIS	2
Fatty acid biosynthesis in <i>E. coli</i> : an overview	2
Model architecture.....	5
Model equations and parameters.....	10
Simulations.....	22
Model adjustment.....	22
Model results.....	24
Summary	27
EXPERIMENTAL PROCEDURES	31
Bacterial strains and growth conditions	31
Preparation of cell extracts.....	32
Western blot	33
LPS quantification.....	34
Phenotypic characterization on agar plates	35
Fatty acid analysis	35
SUPPLEMENTARY RESULTS	36
Overexpression of <i>fabA</i> enhances LpxC degradation	36
Overexpression of <i>waaA</i> is toxic to cells	36
SUPPLEMENTARY REFERENCES	40

MODEL FOR LPS/PHOSPHOLIPIDS BIOSYNTHESIS

Fatty acid biosynthesis in *E. coli*: an overview

Phospholipids are a major and essential component of the bacterial outer membrane. Each molecule consist of a glycerol moiety, a phosphate group, and two fatty acids (except for cardiolipins) (1). Therefore, fatty acid production is essential in outer membrane biogenesis. *E. coli* possesses only three types of phospholipids in its membrane; phosphatidylethanolamine (PE) which comprises the bulk (about 75%), phosphatidylglycerol (PG), and cardiolipin (CL) which represents 15 - 20% and 5 - 10% respectively (1). This section provides only a brief description of reaction steps that occur prior to the commencement of our pathway model (*for detailed description of phospholipids synthesis in E. coli, see reviews (1, 2)*).

The first committed step in *de novo* fatty acid biosynthesis is catalyzed by acetyl-CoA carboxylase (2) (Fig. S1). Acetyl-CoA carboxylase consists of four subunits which form a highly unstable complex (AccABCD); although this complex can be purified as two sub-complexes (3, 4). The reaction requires ATP and two molecules of acetyl-CoA to produce malonyl-CoA. Malonyl-CoA in *E. coli* cells are consumed exclusively in the biosynthesis of fatty acids (1). In addition to the requirement for ATP, each protein subunit must be produced in proportionate amounts thus, acetyl-CoA carboxylase is regulated at the level of transcription (5, 6). Furthermore, acyl-acyl carrier protein (acyl-ACP) inhibits the carboxylase activity presumably to prevent an accumulation of excess acyl-ACPs that may not be required for phospholipids synthesis (7).

Malonyl-CoA is then converted to malonyl-ACP by malonyl-CoA:ACP transacylase (FabD) (Fig. S1). FabD is specific for malonyl-CoA and is incapable of utilizing acetyl-CoA (2). Deletion of this gene is lethal to the cell (8) whereas, overexpression of FabD results in decreased amount of palmitoleic acid and elevated levels of *cis*-vaccenic acid (9). A possible explanation for this observation is that overexpressing FabD would enable malonyl-ACP which has a regulatory effect on FabF to accumulate, and thus, increase the activity of FabF (9). This is because the elongation of palmitoleic acid to *cis*-vaccenic acid is performed exclusively by FabF (10) (Fig. S2). The malonyl-ACP produced is condensed with acyl-

ACPs for fatty acid elongation by the 3-ketoacyl-ACP synthases (**2**). There are three 3-ketoacyl-ACP synthases in *E. coli*; FabB, FabF, and FabH (KASI, KASII, and KASIII) and they are all functionally distinctive.

The initial condensation of malonyl-ACP requires acetyl-CoA and this reaction is performed solely by FabH (**11**) (Fig. S1). Further condensation reactions are conducted exclusively by FabB and FabF which involves the addition of 2-carbon atoms derived from malonyl-ACP to the growing acyl-chain (**2**). The catalytic activities of FabH towards acetyl-CoA and propionyl-CoA are similar and hence, reactions with the latter substrate results in the formation of fatty acids with an uneven number of carbon atoms (**11**). The resulting ketoesters produced by 3-ketoacyl-ACP synthases are reduced by an NADPH-dependent 3-ketoacyl ACP reductase (FabG) (**12**) and the FabG product is further dehydrated by β -hydroxyacyl-ACP dehydratase (FabA and FabZ) (**13**). The final step in the elongation cycle is conducted by enoyl-ACP reductase (FabI) which catalyzes the reduction of reaction products of FabA and FabZ to form an acyl-ACP (**14**). This acyl-ACP in turn, serves as substrate for another condensation reaction. In addition to its dehydratase role, FabA also catalyzes an essential step in the formation of unsaturated fatty acids (UFA). It isomerizes *trans*-2-decenoyl-ACP to *cis*-3-decenoyl-ACP which is essentially the first step towards UFA biosynthesis (**15**).

Long chain acyl-ACPs then serve as substrates for the synthesis of phospholipids resulting from reactions with PlsB, PlsC and other phospholipids enzymes (**1**).

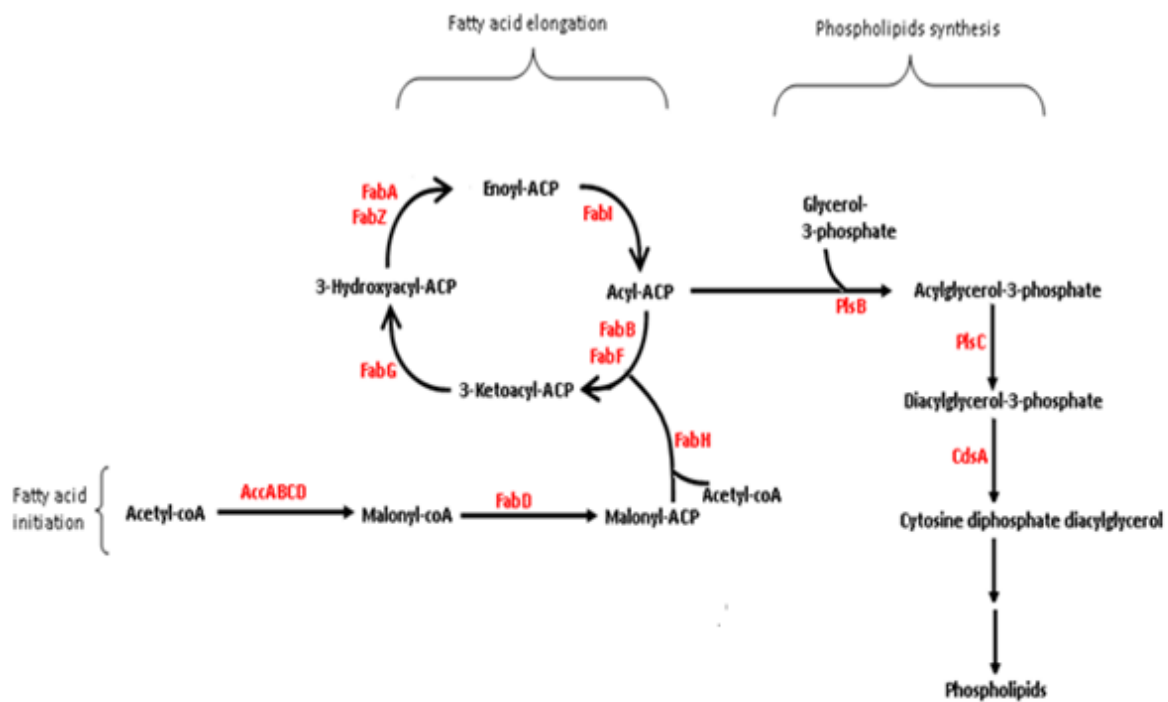


Fig. S1. Schematic representation of phospholipids biosynthesis in *E. coli*. Fatty acid biosynthesis commences with the condensation of two molecules of acetyl-CoA to produce malonyl-CoA which is subsequently converted to malonyl-ACP by FabD. Malonyl-ACP is then condensed with acetyl-CoA by FabH to initiate fatty acids biosynthesis cycle. The role of FabH is solely restricted to fatty acids initiation step. The product of FabH is catalyzed by FabG, FabZ/FabA, and FabI to complete a cycle. The next cycle begins with the condensation of malonyl-ACP with the growing acyl-chain which is catalyzed by FabB/FabF.

Model architecture

A schematic representation of our model is depicted in Fig. S2. Our model commences at fatty acid initiation step with the FabH reaction which then leads to the formation β -hydroxydecenoyl-ACP. This meant that we ignored reaction intermediate steps between the actual product of FabH and β -hydroxydecenoyl-ACP (i.e. the 4-, 6-, and 8-carbon steps). Ignoring these steps was valid since β -hydroxydecenoyl-ACP is a direct substrate for *trans*-2-decenoyl-ACP production. *Trans*-2-decenoyl-ACP in turn, represents a key substrate in the metabolic junction of UFA and saturated fatty acids (SFA) synthesis and our model focuses mainly on the distribution of SFA and UFA moieties present in *E. coli* phospholipids. The consequence of ignoring these steps would have no significant effect on our model output since in reality, perturbation of steps prior to the formation of β -hydroxydecenoyl-ACP would directly affect the pool of *trans*-2-decenoyl-ACP which in turn, would affect both SFA and UFA levels proportionately.

FabH catalyzes the condensation of acetyl-CoA with malonyl-ACP and is not involved in subsequent fatty acid elongation cycle (11). This enzyme is known to be inhibited by acyl-ACPs especially palmitoyl-ACP (C16:0) and *cis*-vaccenoyl-ACP (C18:1) (11).

FabA and FabZ dehydrates β -hydroxydecenoyl-ACP to produce *trans*-2-decenoyl-ACP. Under physiological conditions, this reaction step is unfavourable (13). The *trans*-2-decenoyl-ACP synthesized can either be reduced to decanoyl-ACP (a SFA) by the action of FabI in an essentially irreversible reaction (14), or further isomerized by FabA to produce *cis*-3-decenoyl-ACP which is the first step in UFA biosynthesis (15). Thus, competition for *trans*-2-decenoyl-ACP between FabA and FabI most likely influences the relative ratios of SFA and UFA. However, overexpression of FabA does not increase UFA yield because FabB limits UFA synthesis in this case. In fact, FabA overexpression conditions increased the total cellular SFA whilst the UFA levels remained the same (16). This is because, overexpression would increase the concentration of *trans*-2-decenoyl-ACP, and subsequently result in a faster production of SFA but UFA synthesis rate remain unchanged. Unsurprisingly, overexpression of both FabA and FabB increased the total amount of cellular UFA (17). Decanoyl-ACP and *cis*-3-decenoyl-ACP are both utilized as substrates for further rounds of fatty acyl elongation catalyzed by FabB/FabF, FabG, FabA/FabZ, and FabI respectively.

FabB and FabF differ only in some catalyzed reactions. Both enzymes are capable of catalyzing the elongation of saturated fatty acyl-ACP of chain length C6 to C14 (2). In the synthesis of UFA, FabB catalyzes the condensation of *cis*-3-decenoyl-ACP and *cis*-5-dodecenoyl-ACP. Both FabB and FabF catalyzes *cis*-7-tetradecenoyl-ACP, and the reaction involving palmitoleoyl-ACP is carried out exclusively by FabF (18). Deletion of FabB result in cells that are auxotrophic for UFA (19). On the other hand, overexpression results in increased levels of UFAs (17). FabF is not essential for growth in *E. coli*; however, FabF knockout mutants result in cells that are temperature-sensitive (10). This is because *cis*-vaccenic acid produced from the condensation of palmitoleoyl-ACP is essential at maintaining membrane fluidity under low temperature conditions (2). Overexpression on the other hand, has been reported to be lethal to the cell (20).

One of the key regulation of fatty acid synthesis in *E. coli* is the transcriptional regulation of *fabA* and *fabB* genes (21-23). Both genes have two set of promoters; one which is constitutively expressed, and another which is activated by FadR and repressed by FabR (22, 24-26). Transcription is repressed in the presence of sufficient UFA which further highlights the dual role of FabA and FabB in UFA synthesis (27). In addition to the activation of *fabA* and *fabB*, FadR is also a *repressor* of all genes that code for proteins involved in the β -oxidation cycle (28).

The products of FabB and FabF are reduced by FabG which leads to the formation of a 3-hydroxyacyl ACP. Both unsaturated and saturated fatty acyl substrates* of varying chain-lengths are suitable substrates (12). Under physiological conditions, the reactions are readily reversible (12). Cells are non-viable under FabG knockout conditions which indicate its role cannot be substituted by other enzymes (29).

Next, the 3-hydroxyacyl ACPs are dehydrated by the action of FabA and FabZ; although their substrate preferences differ. This reaction step is unfavourable under physiological

* "*saturated acyl substrate*" was mentioned a number of times in this appendix for certain reactions of FabG, FabB, FabF, FabZ and FabA. Although, only substrates of FabF and FabB can be truly saturated, since all other acyl substrates catalyzed by the enzymes mentioned above always contain at least a double-bond, the term "*saturated acyl substrate*" was utilized for simplicity to represent substrates that are consumed exclusively for SFA synthesis.

conditions as well (13). FabZ prefers acyl substrates of short chain length whereas, FabA has a higher affinity for substrates of medium chain length (13). Unlike FabZ, FabA is incapable of dehydrating acyl-substrates with a *cis* configuration (13). One of the reaction substrates of FabA/FabZ, β -hydroxymyristoyl-ACP is also an essential precursor molecule in the biosynthesis of lipopolysaccharide (LPS) (30) thus, phospholipids and LPS synthesis are regulated in response to perturbation in this common substrate pool (30, 31). Co-ordinated regulation of both pathways is achieved through controlled FtsH-mediated proteolysis of LpxC, the second enzyme involved in LPS synthesis (30, 32). Due to the highly unfavourable equilibrium constant of the first enzyme (LpxA), degradation of LpxC would increase the substrate pool of β -hydroxymyristoyl-ACP. We have postulated previously that the feedback regulatory signal arises from levels of lipid A disaccharide, a metabolite downstream of LpxC in the LPS pathway (33) (*see main article text for more details on LPS/phospholipids regulation*).

An inactivation of the *ftsH* gene is lethal and results in accumulation of LpxC (30). *FtsH* knockout mutants are only viable when a suppressor mutation is present in the *fabZ* gene which encodes a hyperactive FabZ protein (30). Furthermore, Zeng *et al.* (34) isolated cells with mutations in the *fabZ* gene that were resistant to an LpxC inhibitor. The LpxC levels and the catalytic activity of the FabZ protein in these mutants were both decreased. This suggests that the activities of LpxC and FabZ are co-regulated in order to maintain an appropriate ratio of LPS and phospholipids.

The last step catalyzed by FabI is essentially the only irreversible step in the acyl elongation cycle. This enzyme is inhibited by one of its product, palmitoyl-ACP, presumably to prevent an unnecessary accumulation of acyl-ACPs due to the high energy requirement involved in fatty acid synthesis (35). Inhibition of FabI is lethal to the cell (36); however, overexpression does not result in any growth defect (37).

Fatty acid biosynthesis in *E. coli* usually ends when the acyl chain contains 16 or 18 carbon atoms which then serve as substrates for the synthesis of phospholipids (1). The first step in the biosynthesis of phospholipids involves the transfer of two acyl moieties derived from acyl-ACPs to a single molecule of glycerol-3-phosphate (G3P). These acyl groups are attached to G3P by inner membrane proteins PlsB and PlsC (38, 39). Subsequent enzymic

reaction steps occur leading to the formation of membrane phospholipids **(1)**. In our model, we assume that the reaction products of PlsB and PlsC would ultimately be utilized for phospholipids synthesis so we did not model subsequent steps. Thus, our model focuses on the quantification of acyl chains that are transferred to G3P. This was important to effectively study the SFA/UFA distribution in the membrane rather than studying the phospholipid as a whole single molecule. Understanding the relative distributions of SFA/UFA is invaluable because fatty acids are majorly the dynamic and variable component of phospholipids. Also, regulation of the fatty acid composition is crucial under varying environmental conditions.

PlsB attaches fatty acids to position-1 of G3P whereas, fatty acids found in position-2 result from reactions with PlsC **(38, 39)**. Fatty acids located in position-2 are primarily UFA while SFA and *cis*-vaccenic acid are present in position-1 **(38, 39)**. Although myristic (C14:0) and stearic acids (C18:0) can also be detected at significant levels in some *E. coli* strains, the major fatty acids found in *E. coli* membranes are palmitic acid (C16:0), palmitoleic acid (C16:1), and *cis*-vaccenic acids (C18:1) and their ratios vary depending on the bacterial strain and growth conditions **(40)**.

The LPS pathway arm of our model is similar to that which we described previously with some minor modifications **(33)**. We provide a brief summary here.

Biosynthesis of lipid A, the sole essential component of LPS involves nine enzyme catalyzed reaction steps **(41)**. The first enzyme LpxA, is characterized with an unfavourable equilibrium constant of approximately 0.01 which means that LpxC, the second enzyme catalyzes the pathway committed step **(42)**. Pathway regulation occurs through FtsH-mediated degradation of LpxC and WaaA (formerly known as KdtA) **(30, 43)**. In addition, the catalytic activity of LpxK appears to be dependent on the presence of phospholipids especially cardiolipins **(44)**. However, we proposed that the catalytic activation of LpxK is entirely dependent on the abundance of UFA as described below. Our LPS model stops at the MsbA step which meant that enzymic steps involved in LPS transport were ignored. In other words, our model assumes that the rate of LPS transport would not limit the LPS synthesis rate under wild-type conditions.

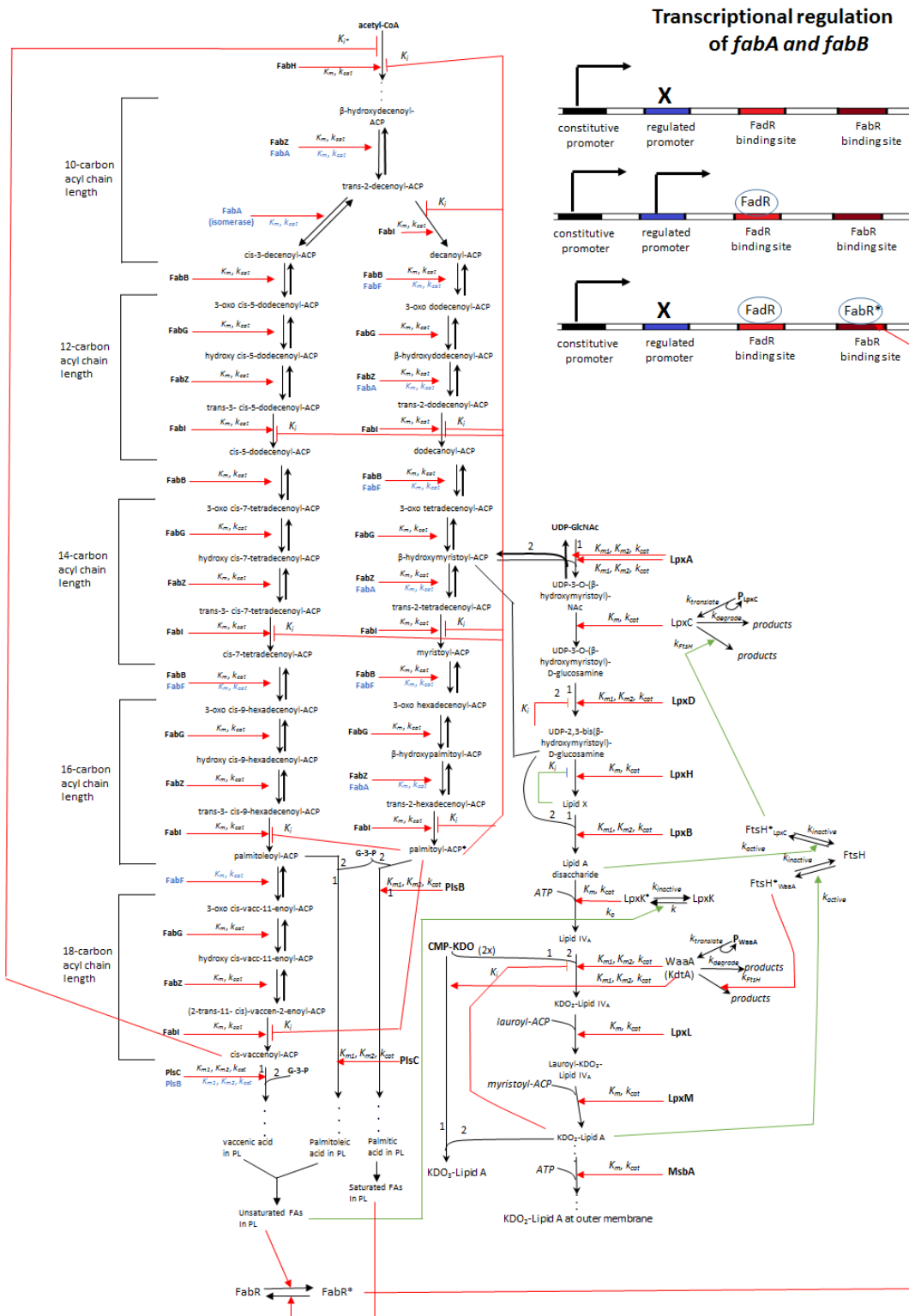


Fig. S2. Model of the *E. coli* LPS and phospholipids biosynthesis pathway. Enzymes and metabolites are shown with three text styles: upright bold indicates that these concentrations

are fixed, upright plain indicates that these concentrations vary, and italics indicates that these species are not included in the model explicitly. Black arrows with barbed heads represent chemical reactions in which reactants are converted to products. Red arrows with closed heads represent enzymatic influences on chemical reaction rates, and red arrows with T-bar heads represent inhibitory influences. Variables represent model parameters. Numbers next to black arrows for bi-substrate reactions show which substrate is designated number 1 and number 2. Green arrows represent pathway interactions that are novel and derived from our previous work, and our current findings. The top right corner shows the transcriptional activation and repression of *fabA* and *fabB* genes. Both genes consist of two separate promoters; one which is constitutively expressed, and another which is activated by FadR and repressed by FabR.

Model equations and parameters

We modelled the interactions between substrates and enzymes under steady-state conditions for an *E. coli* cell. With the exception of FabA, FabB, LpxC and WaaA (whose regulation were being studied in our model), we used a fixed concentration for other proteins thus ignoring protein synthesis and degradation, and cell volume growth. Such assumptions are adequate because enzyme concentrations remain relatively constant over the course of the cell cycle. Table S1 lists all parameters employed in our model.

Substrate and enzyme abundance

We kept the levels of UDP-N-acetylglucosamine (UDP-GlcNAc) and CMP-Kdo constant at 2 million molecules (5 mM) much as we did previously (33). We also maintained the levels of acetyl-CoA and G3P at 2 million and 1 million molecules respectively. This led to substrate saturation conditions throughout our simulations.

The protein counts for LpxA, LpxC, LpxD, LpxH, LpxB, LpxK, WaaA, LpxL, LpxM, FtsH and MsbA were obtained from our previous work (33). We used FabA, FabB, FabF, FabG,

FabH, FabI, FabZ, and FadR protein copy numbers derived from mass spectrometry proteomic data collected on *E. coli* cytosolic fractions (45). We calculated the PlsC count as 4,200 molecules from the reported PlsB count (46) as described below.

Enzyme kinetics

Most of the enzymes involved in fatty acid biosynthesis are involved in multiple reaction steps. This therefore suggests that accounting explicitly for enzyme-substrate complexation is essential. Unfortunately, accounting for complexation requires precise enzyme association/dissociation constant parameters; whereas, available information in the literature indicates the pathway is poorly parameterized. On the other hand, complexation in our model may not be crucial because acyl-ACPs could barely be detected experimentally in *E. coli* cells which indicate their levels are too low (Fig. 8 in (47)). Furthermore, there are a number of thioesterases in *E. coli* which cleave acyl-ACPs and thus, regulate their concentration; although the thioesterases are non-essential (1, 47). Finally, acyl-ACPs in the cytoplasm are toxic to the cell and they induce a strong inhibitory effect on a number of enzymes involved in fatty acid synthesis (11, 35, 48). All these indicate that substrate levels are extremely low and are likely below the K_m value for enzymes. Although acetyl-CoA which is a substrate for FabH is highly abundant in the cell, modelling complexation is unnecessary because FabH is involved in a single-reaction step as mentioned above.

All kinetic parameters for enzymes involved in the LPS biosynthesis arm of our model have been described in our previous work (33). We modelled the phospholipids pathway reactions using either single-substrate or bi-substrate Michaelis-Menten mechanisms. Our integrated LPS/phospholipids model include reversibility of reactions and several feedback loops which are essential for models to attain a steady-state (49).

We employed a single-substrate reversible Michaelis-Menten kinetics for FabG, FabB, FabF, FabZ, and FabA (50). Here the metabolic flux is

$$\frac{d[P]}{dt} = - \frac{d[S]}{dt} = \left(\frac{k_{cat_f} [E][S]}{K_{m_s}} - \frac{k_{cat_r} [E][P]}{K_{m_p}} \right) \left(\frac{1}{1 + \frac{[S]}{K_{m_s}} + \frac{[P]}{K_{m_p}}} \right) \quad (1)$$

where [S] is the substrate concentration, [P] is the product concentration, [E] is the total enzyme concentration, k_{catf} is the enzyme catalytic rate constant for the forward reaction, k_{catr} is the enzyme catalytic rate constant for the reverse reaction, K_{ms} and K_{mp} are the Michaelis constants for substrate and product respectively. The K_{mp} values were unavailable so we assume same values for K_{ms} and K_{mp} in all reversible reactions. This meant that the equilibrium constant for each reaction was implemented by adjusting the k_{catr} parameter as described below.

There were no specific FabG parameters with substrates of carbon chain lengths C10 to C18 so we had to make estimations. The specific activity of FabG whilst utilizing a 4-carbon ketoacyl substrate was reported as 2.9 $\mu\text{mol}/\text{min}/\mu\text{g}$ (51) from which we estimated a k_{cat} value of 1232 s^{-1} , assuming the MW of a FabG protein is 25.5 kDa (52). We assigned this value to k_{catf} for all chain lengths in our model. Furthermore, we utilized a K_m value of 0.01 mM which is the K_m parameter for its second substrate (NADPH) (52). The absence of specific FabG parameters for any of its substrates studied in our model suggests that our model may be inadequate at investigating the effect of FabG perturbations on *E. coli* fatty acid profile. In Toomey and Wakil (12), the FabG reaction led to 40% of substrates being converted to product at a pH of 9.0 (in comparison to the optimum pH of FabG in which all substrates were converted to product). The low product formation was as a result of the reaction becoming unfavourable at a pH of 9.0. However, the physiological pH of *E. coli* is about 7.5 (53), and this led to 70% of products being formed. This suggests that under physiological conditions, the FabG reaction equilibrium constant is 2.3. Since we assume K_{ms} and K_{mp} to be same, this meant that the equilibrium constant equals the k_{catf} / k_{catr} ratio. Thus, we derived k_{catr} as 536 s^{-1} .

We derived the K_m values for FabB with respect to dodecanoyl-ACP (C12:0), myristoyl-ACP (C14:0), *cis*-5-dodecenoyl-ACP (C12:1) and *cis*-7-tetradecenoyl-ACP (C14:1) substrates from Table IV in Garwin *et al.* (54). From the same source, the authors estimated the specific activity of FabB for myristoyl-ACP as 2.9 $\mu\text{mol}/\text{min}/\text{mg}$ from which we estimated k_{catf} as 2.1 s^{-1} . We further derived the k_{catf} values for dodecanoyl-ACP, *cis*-5-dodecenoyl-ACP and *cis*-7-tetradecenoyl-ACP relative to the specific activity for myristoyl-ACP as reported in Garwin *et al.* (54). On the other hand, the catalytic activity of FabB with decanoyl-ACP (C10:0) and dodecanoyl-ACP substrates are similar (18) so we used same K_m and k_{catf} for both substrates.

Although we had initially estimated a FabB k_{cat} value of 14.5 s^{-1} towards *cis*-3-decenoyl-ACP from the reported specific activity in D'Agnolo *et al.* (55), we utilized a k_{cat} of 0.31 s^{-1} as described below.

We obtained FabF parameters for myristoyl-ACP and *cis*-7-tetradecenoyl-ACP from Table IV in Garwin *et al.* (54) much as we did for FabB. According to Figure 3 in Edwards *et al.* (18), we estimated that the catalytic activity of FabF whilst utilizing decanoyl-ACP and dodecanoyl-ACP substrates was 3.6 and 3.25 folds higher respectively relative to myristoyl-ACP. We implemented this fold increase by adjusting the k_{catf} values relative to those of myristoyl-ACP while maintaining same K_m values. Furthermore, we derived the equilibrium constant of the FabB and FabF reactions as 9 and 1.86 respectively from Figure 3 in D'Agnolo *et al.* (55) much as we did for FabG, which enabled us to estimate k_{catr} parameters.

We estimated a k_{catf} value of 0.53 s^{-1} from the reported specific activity of FabZ towards β -hydroxymyristoyl-ACP (C14:0) (34). There were no available K_m parameters for FabZ so we had to make estimations as well. In Zeng *et al.* (34), the authors found that in a $40 \mu\text{l}$ reaction volume, varying the concentration of FabZ from 12.75 to 25.5 nM resulted in a specific activity of $1.87 \mu\text{mol}/\text{min}/\text{mg}$ when the concentration of β -hydroxymyristoyl-ACP was $50 \mu\text{M}$. Since the specific activity of a reaction equals the rate of reaction multiplied by reaction volume, divided by the mass of total protein, we can estimate the reaction rate in their experiments and subsequently derive K_m . If we assume an enzyme concentration of 12.75 nM, this amounts to $8.67 \times 10^{-6} \text{ mg}$ in $40 \mu\text{l}$ (MW of FabZ is 17 kDa) thus, we can calculate the reaction rate R, as $6.75 \times 10^{-3} \mu\text{M}/\text{s}$. The K_m constant can then be derived from $R = \frac{k_{cat} [E][S]}{K_m + [S]}$. By inputting the necessary parameters ($[E] = 12.75 \text{ nM}$, $k_{cat} = 0.53$, $[S] = 50 \mu\text{M}$), we estimated K_m as $5.5 \times 10^{-5} \text{ mM}$. We utilized this K_m value for all substrates of FabZ. Furthermore, we calculated the k_{catf} values for β -hydroxydecanoyl-ACP (C10:0), β -hydroxydodecanoyl-ACP (C12:0) and β -hydroxypalmitoyl-ACP (C16:0) relative to that of β -hydroxymyristoyl-ACP according to Figure 5 in (13).

The specific activity of FabZ whilst catalyzing β -hydroxy-*cis*-7-tetradecenoyl-ACP (C14:1) is similar to that of β -hydroxymyristoyl-ACP (Figure 6 in (13)). Consequently, the parameters for FabZ were same for both substrates in our model. There were no available information in the literature to estimate parameters for other *cis*-unsaturated acyl substrates of

FabZ. We assumed similar rates for both saturated and *cis*-unsaturated acyl substrates of the same chain length. This meant that parameters for 12-carbon and 16-carbon saturated substrates were assigned to 12-carbon and 16-carbon *cis*-unsaturated substrates respectively.

The reaction affinity of FabA and FabZ towards β -hydroxymyristoyl-ACP is also similar (13). Since they both have similar molecular weight, this indicates they also share similar k_{catf} values as well. We calculated the FabA k_{catf} values for β -hydroxydecanoyl-ACP, β -hydroxydodecenoyl-ACP and β -hydroxypalmitoyl-ACP relative to β -hydroxymyristoyl-ACP according to Figure 5 in (13). We obtained a FabA K_m value of 1.7 mM for β -hydroxydecanoyl-ACP from Kass *et al.* (15). This K_m value was assigned to other β -hydroxy substrates of FabA.

The equilibrium constant for the dehydratase activity (i.e FabZ and FabA) has been reported to vary with substrate chain length. Under reactions involving short chain substrates (4-carbon chain), the ratio of substrates to products was 1:9 indicating the reverse reaction is more favourable (14). However, the ratio of substrates to product becomes 75:22 (the unaccounted 3% is the *cis*-product from the FabA isomerase reaction which indicates the equilibrium constant for the isomerase reaction is 0.14) when utilizing β -hydroxydecanoyl-ACP as substrate indicating an equilibrium constant of 0.29 (13). We can therefore calculate the k_{catr} values of FabA and FabZ for this substrate. Furthermore, the substrate/product ratio becomes 1:1 under reactions involving long chain substrates (14). This meant that k_{catf} and k_{catr} for all other dehydratase reactions were same.

For the isomerase activity of FabA, we estimated the k_{catr} as 11.7 s^{-1} (i.e. *cis*-3-decenoyl-ACP was substrate) from Figure 7 in (56) and obtained the K_{mp} parameter from Kass *et al.* (15). The reaction equilibrium constant of 0.14 as mentioned above enabled us to derive k_{catf} . Although we initially assumed same values for K_{ms} and K_{mp} , we utilized a K_{ms} value of 0.0001 mM as described below.

We used bi-substrate Michaelis-Menten kinetics for the transfer of fatty acyl moieties to G3P by PlsB and PlsC. Here, the metabolic flux is

$$\frac{d[P]}{dt} = -\frac{d[S_1]}{dt} = -\frac{d[S_2]}{dt} = \frac{k_{cat}[E][S_1][S_2]}{(K_{m_1} + [S_1])(K_{m_2} + [S_2])} \quad (2)$$

where $[S_1]$ and $[S_2]$ are the two substrate concentrations with respective Michaelis-Menten constants K_{m1} and K_{m2} . The phospholipid fatty acid composition in our model only includes the major fatty acids found in *E. coli* membranes (i.e. palmitic, palmitoleic, and *cis*-vaccenic acids). This is because other minor fatty acids vary from strain-to-strain and sometimes, non-existent in some *E. coli* strains. As mentioned above, PlsB and PlsC attaches fatty acids to positions-1 and -2 of G3P respectively. Fatty acids found in position-1 are palmitic and *cis*-vaccenic acids while palmitoleic and, again, *cis*-vaccenic acids are present in position-2. Hence, PlsB and PlsC both utilize *cis*-vaccenoyl-ACP.

We derived the PlsB k_{cat} values from the reported specific activities of 9.5 and 8.5 $\mu\text{mol}/\text{min}/\text{mg}$ for palmitoyl-ACP and *cis*-vaccenoyl-ACP substrates respectively (46).

There were no available specific k_{cat} and K_m values for PlsC so we had to make estimations as well. Rock *et al.* (39) reported a K_m value of 0.012 mM for the incorporation of palmitoleoyl-ACP into G3P whilst using inner membrane enzymic fractions. Since incorporation of palmitoleoyl-ACP is conducted exclusively by PlsC, we can assign this K_m value to PlsC with the assumption that there was no competition for this substrate with other membrane proteins. The authors also reported similar specific activities for the incorporation of palmitoyl-ACP and palmitoleoyl-ACP. The incorporation of palmitoyl-ACP is also performed exclusively by PlsB. This therefore suggests that 1 mg of inner membrane fraction (which contains PlsB) whilst utilizing palmitoyl-ACP would result in the same reaction rate as 1 mg of inner membrane fraction (containing PlsC) when catalyzing palmitoleoyl-ACP. Since the molecular weight of PlsB is 3 times that of PlsC (46, 57), this suggests that the PlsC copy number in membrane extract is 3 times that of PlsB (hence, PlsC count per cell is about 4200 molecules). This also suggests that the k_{cat} value for PlsC towards palmitoleoyl-ACP would be 3 times less than that for PlsB with palmitoyl-ACP substrate.

Additionally, Goelz and Cronan (38) observed that 32% of fatty acids attached to position-1 of G3P were *cis*-vaccenic acids (i.e. by PlsB). We ran initial simulations for PlsB using COPASI (50) (1400 copies per cell (46)) with saturation levels of palmitoyl-ACP and *cis*-vaccenoyl-ACP and parameters described above. We observed that when there was no competition for *cis*-vaccenoyl-ACP (i.e. absence of PlsC), 37% of fatty acids attached to position-1 were *cis*-vaccenic acid instead of 32%. However, when competition was included

(i.e. presence of PlsC), we observed the V_{max} for PlsC required to attain 32% of *cis*-vaccenic acid in position-1 was 1.94 folds greater than that of PlsB. Thus, with the knowledge of the PlsB k_{cat} value for *cis*-vaccenoyl-ACP, and protein counts for both PlsB and PlsC, we can derive the k_{cat} of PlsC towards *cis*-vaccenoyl-ACP substrate as 7.6 s^{-1} .

We used single-substrate Michaelis-Menten kinetics with inhibition for the FabI enzyme for all substrates. In this case, the metabolite flux is

$$\frac{d[P]}{dt} = -\frac{d[S]}{dt} = \frac{k_{cat}[E][S]}{(K_m + [S])\left(1 + \frac{[P]}{K_i}\right)} \quad (3)$$

where K_i is the inhibition constant, [P] is the concentration of palmitoyl-ACP, and the other parameters are the same as in eq. 2.

We used same parameters for *trans*-2-tetradecenoyl-ACP (C14:0) and *trans*-2-dodecenoyl-ACP (C12:0) since they both had similar affinities with FabI (58). There was no information in the literature regarding FabI reactions with *trans*-2-hexadecenoyl-ACP (C16:0). We assumed that the FabI reaction rate would not increase with increasing carbon-chain length for saturated substrates since the affinities of *trans*-2-dodecenoyl-ACP and *trans*-2-tetradecenoyl-ACP were same. Furthermore, in the absence of FabI parameters with *cis*-unsaturated substrates, we assigned same parameters for saturated 12-carbon, 14-carbon and 16-carbon substrates to 12-carbon, 14-carbon and 16-carbon *cis*-unsaturated substrates respectively. We estimated the FabI k_{cat} value for *trans*-2-decenoyl-ACP from Figure 7 in Weeks and Wakil (58) relative to that reported for *trans*-2-dodecenoyl-ACP in Rafi *et al.* (59) and also derived its K_m parameter relative to *trans*-2-dodecenoyl-ACP from Figure 6 of (58). Finally, Heath and Rock (35) observed that at a palmitoyl-ACP concentration of 400 μM , the FabI reaction rate was inhibited by 92%. If we assume non-competitive inhibition and excess substrate conditions, we can derive the K_i value as 0.035 mM.

We modelled the FabH reaction step using an irreversible single-substrate Michaelis kinetics with dual acyl-ACP (palmitoyl-ACP and *cis*-vaccenoyl-ACP) inhibition. Here, the metabolite flux is

$$\frac{d[P]}{dt} = -\frac{d[S]}{dt} = \frac{k_{cat}[E][S]}{(K_m + [S])\left(1 + \frac{[P]}{K_i}\right)\left(1 + \frac{[P^*]}{K_{i^*}}\right)} \quad (4)$$

where K_{i^*} is inhibition constant arising from *cis*-vaccenoyl-ACP ($[P^*]$) and other parameters are same as eq. 3.

We initially derived the FabH k_{cat} value of 3.28 s^{-1} from the reported specific activity (11) but knew at this point that this parameter would be insufficient to produce sufficient β -hydroxydecanoyl-ACP for SFA and UFA synthesis (the FabH molecule count is 1320 per cell (45) which suggests a maximum production of 8 million products whereas, approximately 20 million fatty acids are generated *in vivo* (41)). This is unsurprising as it has been suggested previously that there are other enzymes capable of replacing FabH (60). Consequently, we increased the k_{cat} value to 12 s^{-1} . We estimated the inhibition constants for palmitoyl-ACP and *cis*-vaccenoyl-ACP inhibitors as 0.1 mM and 0.067 mM from Heath and Rock (11) much as we did for FabI above.

LpxK catalytic activation and inactivation

We modelled the activation of LpxK from an inactive to an active state using mass action kinetics according to

$$\frac{d[LpxK^*]}{dt} = k \left(1 + \frac{[\text{activator}]}{K_a}\right) [LpxK] - K_{inact}[LpxK^*] \quad (5)$$

where k is the phospholipids-independent activation constant, K_a is the phospholipids-dependent activation constant, K_{inact} is the inactivation constant, [activator] is the phospholipids concentration (i.e. fatty acids), $[LpxK^*]$ and $[LpxK]$ represent the concentrations of the activate and inactive forms of LpxK.

In Ray and Raetz (44), the absence of phospholipids resulted in a maximum reaction rate which was 94% less than those with phospholipids stimulation. Since there are about 432 copies of LpxK per cell (33), this means the absence of phospholipids would result in 406

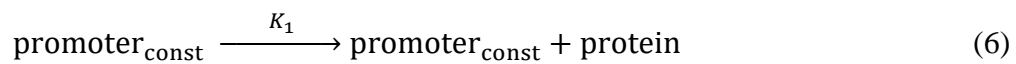
copies of inactive LpxK and 26 copies of active LpxK. We assumed K_{inact} to be 0.1 s^{-1} and subsequently derived k as 0.0064 s^{-1} .

When cells newly divide, LpxK would most likely be maximally activated quickly due to the essential need for LPS production. We assume that this maximal activation (which we arbitrarily defined as 95% of active proteins) would occur within 100 s. We also assume that about 1.1×10^6 fatty acids would have been produced in 100 s. This is because, there are approximately 1 million LPS in *E. coli* (41) and the LPS/phospholipids ratio is about 0.1 (41, 61). Since 2 molecules of fatty acids make up a phospholipid molecule (with the exception of cardiolipins which occupy about 5% of total phospholipids), this suggests approximately 20 million fatty acids are produced for phospholipid biosynthesis per generation time. Thus, in 100 s, approximately 1.1×10^6 fatty acids would be synthesized assuming a cell generation time of 30 min. By Inputting LpxK and LpxK* counts as 22 and 410 molecules respectively, coupled with the activator concentration, we can derive K_a as 0.0094 mM.

Transcriptional regulation of fabA and fabB

The expression of *fabA* and *fabB* genes occur from two different promoters. One of them which is usually regarded as the ‘weak promoter’ is constitutive while the dominant promoter is regulated through mediated transcriptional activation and repression by FadR and FabR proteins respectively.

We modelled protein synthesis from the constitutive promoter according to the zeroth order reaction



where $\text{promoter}_{\text{const}}$ represents the constitutive promoter and K_1 is the resulting protein translation rate constant. This approach combines transcription and translation into a single reaction step.

When FadR and FabR are inactivated, protein expression would occur solely from the constitutive promoter. Feng and Cronan (25) observed that mRNA levels of *fabA* were 40% those of wild-type cells while those for *fabB* remained the same in a *fadR* and *fabR* double mutant. We assume that the relative fold-reduction in mRNA levels would result in a similar

fold-reduction in protein levels. This is a reasonable assumption since neither FabA nor FabB are regulated at the post-transcription or post-translation level. Therefore, the transcript half-lives, protein translation and degradation rates would remain constant under FabR and FadR inactivation conditions. In wild-type *E. coli*, the FabA count is 23,400 (45) which indicates a *fadR/fabR* double mutant contains approximately 9,360 FabA proteins. Thus, we can derive the translation rate as the production of 9,360 proteins over the course of a cell generation which gives a K_I of 5.2 molecules/s (assuming a generation time of 30 min). On the other hand, there are 14,300 FabB proteins per cell which enabled us to derive K_I as 7.945 molecules/s.

In order to induce expression *fabA* and *fabB* expression, FadR is likely to be activated. We modelled the activation of FadR from an inactive to an active state using first order reaction kinetics



where [FadR] and [FadR*] are the inactive and active forms of FadR, K_2 and K_{-2} are the resultant activation and inactivation constants respectively. The cellular count of FadR is about 295 (45). We assume 100 copies of these would be used in the regulation of *fabA* and *fabB* (in which case, [FadR*] = 100) thereby leaving a reasonable FadR reservoir for other regulatory processes. This estimate may be inaccurate; however, they do not affect the model results at all. Thus, the estimate is only necessary to capture the activation of FadR. We also assumed K_{-2} as 0.1 s^{-1} which then gave a K_2 value of 0.054 s^{-1} . Again, the accuracy of the K_2 and K_{-2} values are inconsequential provided their ratios are accurate.

The activated form of FadR can bind reversibly to a DNA sequence downstream the regulated promoter and induce protein expression.

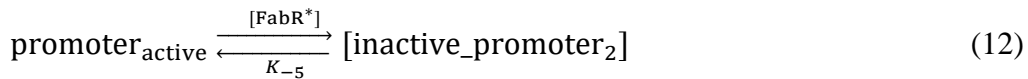


where $\text{promoter}_{\text{reg}}$ is the regulated promoter, $\text{promoter}_{\text{active}}$ is the active promoter resulting from FadR binding to DNA sequence, K_{active} and K_{inactive} are the resultant activation and inactivation constants. K_3 is the translation rate constant from the activated promoter.

As mentioned above, there are 23,400 FabA proteins in wild-type *E. coli*. This means that the sum of K_I and $[\text{promoter}_{\text{active}}]K_3$ equals the synthesis of 23,400 proteins per cell generation time. There are four different states the regulated promoter can assume in our model; (i) an inactive state resulting from lack of DNA binding by FadR or FabR; (ii) an active state from DNA binding by FadR; (iii) an inactive state arising from FabR bound to DNA; and (iv) an inactive state arising from DNA binding by FabR in addition to a bound FadR. Irrespective of FadR bound to DNA, binding of FabR would prevent expression (27). The FabR and FadR concentrations are likely to be optimized for precise control, so we assumed that their concentrations are about half of the binding constant values. This implies that the probability is 0.25 for each of the 4 states. This meant that $[\text{promoter}_{\text{active}}]$ count equals 0.25. Inputting this value with prior estimate of K_I resulted in a K_3 value of 31.2 s^{-1} . Furthermore, the transcript levels for *fabA* were increased by 1.8 folds in a *fabR* mutant which we estimated would result in 42,120 proteins. This indicates that there was continuous expression from the regulated promoter which meant the promoter can achieve only two possible states. Again, with prior knowledge of K_I and K_3 , we can estimate $[\text{promoter}_{\text{active}}]$ as 0.583 molecules in a *fabR* mutant and subsequently derive $[\text{promoter}_{\text{reg}}]$ as 0.417 molecules. Next, assuming K_{inactive} as 0.1 s^{-1} , coupled with the $[\text{FadR}^*]$, $[\text{promoter}_{\text{reg}}]$, and $[\text{promoter}_{\text{active}}]$ values, we can derive K_{active} as $1.4 \times 10^{-3} \text{ s}^{-1}$.

On the other hand, the expression rates of *fabB* were similar in both wild-type and *fadR* mutant (25) which suggest FabR is the dominant regulator of *fabB*. This indicates that in wild-type cell, expression occurs mainly from the constitutive promoter which gives the $[\text{promoter}_{\text{active}}]$ count as approximately zero. However, in a *fabR* mutant, the mRNA levels were increased by 1.7 folds in comparison to wild-type (25) which we estimate would lead to 24,310 FabB proteins. Yet again, only two possible promoter states exist under *fabR* inactivation conditions and we assume $[\text{promoter}_{\text{reg}}]$ and $[\text{promoter}_{\text{active}}]$ as both 0.5 molecules each. This enabled us to derive K_{active} as $1.0 \times 10^{-3} \text{ s}^{-1}$ much as we did for *fabA*.

The activation of FabR from an inactive to an active state is stimulated by the presence of UFA (27). It is believed that the cell is able to detect the relative ratio of SFA and UFA which then determines if FabR is activated (27). The activated form of FabR then binds to an overlapping DNA sequence downstream of FadR (27). Prior binding of FadR does not prevent the binding of FabR. Therefore, an active form of FabR can bind to DNA with different promoter states of [promoter_{reg}] and [promoter_{active}] to give two different promoter inactive states.



where [FabR] and [FabR*] are the inactive and active forms of FabR, [UFA] and [SFA] are the concentrations of UFA and SFA respectively, [inactive_promoter₁] and [inactive_promoter₂] are the different inactive promoter states, K_{-4} and K_{-5} are the FabR dissociation rate constants from DNA of [inactive_promoter₁] and [inactive_promoter₂] respectively. There were no specific estimates for the FabR cellular count in the literature so we assumed same count as FadR. We also assume that the affinity of active FabR for promoter_{reg} and promoter_{active} are similar which meant that the FabR dissociation constant is same irrespective of the promoter state. We derived the K_{-4} and K_{-5} parameters during model fitting.

We modelled protein degradation with first order kinetics as well, with K_{degrade} as the degradation rate constant. The steady-state protein abundance in a cell is $(K_I + [\text{promoter}_{\text{active}}] * K_3) / K_{\text{degrade}}$. We estimated a K_{degrade} value of $5.556 \times 10^{-4} \text{ s}^{-1}$ for FabA and FabB using [promoter_{active}], K_I and K_3 parameters described above.



Simulations

We simulated our LPS and phospholipids synthesis model using deterministic methods. Our primary tool was the COPASI software (50). We assumed a 6.7×10^{-16} litre cell volume (62). Our simulations represented an *E. coli* cell generation under optimal growth conditions which is 1800 s (63). We have identified previously (33) that using stochastic simulations and accounting for stochasticity had negligible effect on the results due to the high copy numbers of all model components which justified the use of deterministic simulations. Our model has been deposited in the BioModels database and assigned the identifier MODEL1601080000.

Model adjustment

Our initial model parameters described above were unable to either achieve the appropriate SFA/UFA ratio or replicate some published experimental findings. This was as a result of limitations in the following areas;

FabA isomerase and FabZ kinetics

Initial simulations resulted in excess SFA and little or no UFA. This was solely due to FabI outcompeting FabA isomerase for *trans*-2-decenoyl-ACP substrate which led to an accumulation of SFA substrates. We solved this problem by reducing the K_{ms} value of FabA isomerase towards *trans*-2-decenoyl-ACP to 0.0001 mM which resulted in SFA occupying 50% of total fatty acids. Indeed, there were no reported K_m parameters for the isomerization of *trans*-2-decenoyl-ACP in the literature so it is unsurprising that our initial estimate was inadequate.

Although we had obtained 50% SFA yield, a bottleneck in the UFA arm of the pathway ensured an insufficient production of UFA resulting from accumulation of substrates of FabZ. Again, this is understandable given there were also no reported parameters for *cis*-unsaturated substrates of FabZ in the literature as mentioned earlier. We resolved this problem by increasing both the k_{catf} and k_{catr} parameters (so the equilibrium constant remained the same) for the 14, 16 and 18-carbon unsaturated substrates by 3 folds.

FabB activity towards cis-3-decenoyl-ACP

Our initial parameters were unable to reproduce the roles of FabA and FabB in the synthesis and regulation of UFA. For instance, overexpressing *fabA* in our model resulted in increased levels of UFA rather than the opposite effect. This was solely due to the high affinity of FabB for *cis*-3-decenoyl-ACP. This then suggests that the specific activity of FabB *in vivo* is far less than those reported *in vitro* by D’Agnolo *et al.* (55). There are several pieces of evidence that supports the claim of FabB being the rate-limiting step in UFA synthesis. Firstly, overexpression of *fabA* (which will theoretically increase the concentration of *cis*-3-decenoyl-ACP) does not increase nor decrease UFA yield, although SFA levels are elevated (16). Secondly, overexpression of *fabB* enhances UFA yield (17). In order to ensure FabB was the rate-limiting step in UFA synthesis, we decided to decrease the k_{catf} parameter for *cis*-3-decenoyl-ACP substrate. The proportion of SFA in wild-type *E. coli* under optimum conditions ranges from 50 – 70% of the total fatty acids (27, 64). Whilst the levels of FabA and FabB were fixed to their steady-state counts, we decided to reduce the k_{catf} value so that our model would produce 60% SFA, which turned out to be a value of 0.31 s^{-1} .

LpxK catalytic activation

At first, when we investigated the role of fatty acid biosynthetic enzymes on LpxC regulation, our model results deviated from published datasets. For instance, our model inhibition of FabZ did not result in LpxC degradation in contrast to experimental findings by Zeng *et al.* (34). This was because our model had sufficient amount of fatty acids (especially SFA) to catalytically activate LpxK which ensured that lipid A disaccharide (the feedback source for LpxC degradation) did not accumulate. However, when we made the catalytic activation of LpxK to arise solely from UFA, we were able to replicate the results in Zeng *et al.* (34), other published results, and our subsequent experimental findings (presented in the main article text). Thus, the activation of LpxK is most likely sensitive to the SFA/UFA ratio. We modified eq. 5 to ensure LpxK was catalytically activated by UFA and inactivated by SFA.

$$\frac{d[\text{LpxK}^*]}{dt} = k \left(1 + \frac{[\text{UFA}]}{K_a} \right) [\text{LpxK}] - K_{inact}[\text{SFA}][\text{LpxK}^*] \quad (14)$$

where [UFA] and [SFA] are the concentrations of the activator and deactivators respectively and other parameters are same as in eq. 5. Here we assume $K_{inact}[\text{SFA}]$ equals 0.1 s^{-1} . As
23

mentioned above, wild-type cells contain about 20 million fatty acids and 60% of these comprise of SFA which is 12 million copies (29.7 mM). Using this concentration, we can derive K_{inact} as $0.0034 \text{ mM}^{-1}\text{s}^{-1}$.

As we stated in the main article text, Ray and Raetz (44) observed that activation of LpxK by other fatty acids was much less in comparison to cardiolipins. The authors made use of bovine heart cardiolipins and these are known to contain at least 94% UFA of the total fatty acids (65).

Finally, we fitted the $K_{.4}$ and $K_{.5}$ values as 90 s^{-1} for *fabA*, and 2 s^{-1} for *fabB* which resulted in a protein steady-state count.

Model results

FabZ inhibition and overexpression

Zeng *et al.* (34) isolated FabZ mutants with decreased specific activities that had low levels of LpxC. The authors also observed that overexpression of FabZ increased levels of LpxC in wild-type cells. Although there were no specific LpxC fold changes in either case from Zeng *et al* to quantitatively make comparison, we tested both perturbations in our refined model by decreasing or increasing the FabZ counts by 100 folds. As presented in Fig. S3A, LpxC levels were decreased by 40% when FabZ was inhibited and consequently, the amount of LPS being produced was also reduced by 40%. We observed the LpxK catalytic activation rate was reduced by 50% which enabled lipid A disaccharide to accumulate and negatively feedback on LpxC degradation. Our model strain had excess SFA and could barely synthesize UFA due to the absence of an essential FabZ role at dehydrating *cis*-containing β -hydroxyacyl-substrates. Despite this, we observed no accumulation of FabZ substrates due to the readily reversible nature of the FabZ reactions. However, the production of SFA was able to occur because FabA was active. Nevertheless, the dehydratase role of FabZ in UFA synthesis cannot be complemented by FabA (13). We also observed an upregulation in FabA and FabB concentrations but these had no effect at elevating the concentrations of UFA because FabZ became the rate-limiting step.

On the other hand, the steady-state concentration of LpxC was increased by 2.6 fold when FabZ was overexpressed in our model (Fig. S3A). However, we observed LPS levels were reduced by 70%. Since cells become non-viable when LPS amounts are reduced by more than 50% (66), overexpression of FabZ would result in a lethal effect to the cell in agreement with data presented in Zeng *et al.* (34). Regarding the fatty acid profile, the production of SFA was slightly enhanced while UFA amounts remained the same. Although Lee *et al.* (67) had reported that overexpression of FabZ increases the proportion of UFA, their data exhibited this phenomenon only after prolonged growth (i.e. stationary phase) whereas, our model represents the exponential or steady-state growth phase of *E. coli*. In fact, their results indicated that when the cells were harvested early, SFA was increased and UFA decreased. Thus, in this respect, our FabZ model is compatible with their experiments. Despite the slight increase in SFA levels in our model, we did not observe an up-regulation of FabA or FabB.

The role of FabA and FabB in UFA biosynthesis

As mentioned above, cellular requirement for UFA results in an upregulation of both *fabA* and *fabB* genes which enhances UFA yield. However, sole overexpression of *fabA* increases SFA synthesis rather than UFA synthesis (16, 17). We tested this phenomenon in our model as presented in Figure S3B. Our model results agree qualitatively with experimental evidence presented in Clark *et al.* (16). The slight quantitative disparity may arise since the experimental results used for comparison were carried out at 42°C whereas, our model parameters represent optimum conditions. Alternatively, the quantitative differences could arise due to strain-to-strain fatty acids variability.

Overexpression of FabH

In Tsay *et al.* (68), it was shown that overexpression of FabH increased the cellular concentration of SFA by 16%. Testing this perturbation in our model was relatively straightforward. We observed a 10% increase in SFA levels when the FabH count was increased by 100 folds in close agreement with the experiments. Furthermore, our model showed an increase in the expression levels of FabA and FabB; however, expression of the latter was not as pronounced as FabA.

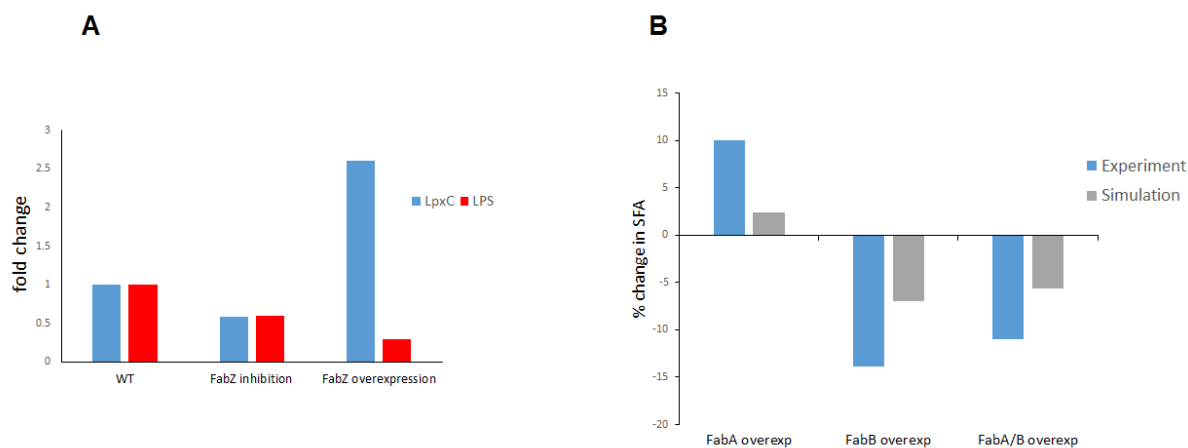


Fig. S3. Model results. Model conditions were those depicted in Fig. S2 and using parameters presented in Table S1. **(A)** Effect of FabZ inhibition and overexpression on LpxC and LPS levels. The FabZ molecule count was increased or decreased by 100 folds to represent FabZ overexpression and inhibition respectively. **(B)** The role of FabA and FabB on SFA/UFA ratio. The FabA and FabB counts were kept constant and increased by 100 folds to represent overexpression conditions. This meant that FadR/FabR regulation was disabled.

Summary

We have developed a computational model for the outer membrane of *E. coli*, drawing parameters from the literature, and making estimates where possible. Our model agrees qualitatively with experimental data and to some extent, quantitatively. However, our model may be inadequate for testing certain pathway perturbations. For instance, there were no specific parameters for FabG for any of the substrates studied in our model so our estimate may only be adequate under wild-type conditions where FabG does not limit pathway flux. Also, as stated above, FadR is a global regulator of certain genes involved in fatty acid biosynthesis and degradation. Apart from the transcriptional activation of *fabA* and *fabB*, the other roles of FadR are outside the scope of our work hence, our model may be inappropriate at studying the effect of FadR dynamics on fatty acid synthesis.

Table S1: Abundance and kinetic parameters of integrated LPS and phospholipids biosynthesis model.

Species	Species abundance (molec./cell)	Substrate	Substrate identity in the SBML file	K_{ms} or K_m (mM)	K_{mp} (mM)	k_{cat} or k_{catf} (s^{-1})	k_{catr} (s^{-1})	Notes and other parameters
UDP-GlcNAc	2,000,000							excess concentration
CMP-Kdo	2,000,000							excess concentration
G3P	1,000,000							excess concentration
Acetyl-CoA	2,000,000							excess concentration
ACP	1,024 ^a							actual concentration
FabH	1,320 ^a			0.04 ^g		12		$K_i = 0.1$ mM $K_{i^*} = 0.067$ mM
FabB	14,300 ^a	Decanoyl-ACP	C10	0.022	0.022	3.4	0.38	$K_I = 7.965$ s ⁻¹
		Dodecanoyl-ACP	C12	0.022 ^c	0.022	3.4	0.38	$K_{active} = 1.0 \times 10^{-3}$ s ⁻¹
		Myristoyl-ACP	C14	0.071 ^c	0.071	2.1	0.23	$K_{inactive} = 0.1$ s ⁻¹
		<i>cis</i> -3-decenoyl-ACP	C10:1	0.012 ^d	0.012	0.31	1.6	$K_3 = 11.12$ s ⁻¹
		<i>cis</i> -5-dodecenoyl-ACP	C12:1	0.028 ^c	0.028	3.9	0.43	$K_{.4} = 2$ s ⁻¹
		<i>cis</i> -7-tetradecenoyl-ACP	C14:1	0.027 ^c	0.027	4.14	0.46	$K_{.5} = 2$ s ⁻¹
								$K_{degrade} = 5.556 \times 10^{-4}$ s ⁻¹
FabF	1,280 ^a	Decanoyl-ACP		0.068	0.068	3	1.6	
		Dodecanoyl-ACP		0.068	0.068	2.7	1.45	
		Myristoyl-ACP		0.068 ^c	0.068	0.83	0.45	
		<i>cis</i> -7-tetradecenoyl-ACP		0.06 ^c	0.06	2.49	1.34	
		Palmitoleoyl-ACP	C16:1	0.017 ^d	0.017	6.74 ^d	3.6	
FabG	13,800 ^a	3-oxo-dodecenoyl-ACP	Ketoacyl-12	0.01	0.01	1232	536	
		3-oxo tetradecenoyl-ACP	Ketoacyl-14	0.01	0.01	1232	536	
		3-oxo hexadecenoyl-ACP	Ketoacyl-16	0.01	0.01	1232	536	
		3-oxo- <i>cis</i> -5-dodecenoyl-ACP	Ketoacyl-12:1	0.01	0.01	1232	536	
		3-oxo- <i>cis</i> -7-tetradecenoyl-ACP	Ketoacyl-14:1	0.01	0.01	1232	536	
		3-oxo- <i>cis</i> -9-hexadecenoyl-ACP	Ketoacyl-16:1	0.01	0.01	1232	536	

		3-oxo- <i>cis</i> -vacc-11-enoyl-ACP	Ketoacyl-18:1	0.01	0.01	1232	536	
FabZ	3,330 ^a	β -hydroxydeceoyl-ACP	B-OH-10	5.5×10^{-5}	5.5×10^{-5}	2.65	9.14	
		β -hydroxydodeceoyl-ACP	B-OH-12	5.5×10^{-5}	5.5×10^{-5}	1.59	1.59	
		β -hydroxymyristoyl-ACP	Beta-hydroxymyristoylACP	5.5×10^{-5}	5.5×10^{-5}	0.53	0.53	
		β -hydroxypalmitoyl-ACP	B-OH-16	5.5×10^{-5}	5.5×10^{-5}	1.06	1.06	
		β -hydroxy- <i>cis</i> -5-dodeceoyl-ACP	B-OH-12:1	5.5×10^{-5}	5.5×10^{-5}	1.59	1.59	
		β -hydroxy- <i>cis</i> -7-tetradecoyl-ACP	B-OH-14:1	5.5×10^{-5}	5.5×10^{-5}	1.59	1.59	
		β -hydroxy- <i>cis</i> -9-hexadecoyl-ACP	B-OH-16:1	5.5×10^{-5}	5.5×10^{-5}	3.18	3.18	
		β -hydroxy- <i>cis</i> -vacc-11-enoyl-ACP	B-OH-18:1	5.5×10^{-5}	5.5×10^{-5}	3.18	3.18	
FabA	23,400 ^a	β -hydroxydeceoyl-ACP		1.7 ^e	1.7	5.4	18.6	$K_I = 5.2 \text{ s}^{-1}$
		β -hydroxydodeceoyl-ACP		1.7	1.7	4	4	$K_{activate} = 1.4 \times 10^{-3} \text{ s}^{-1}$
		β -hydroxymyristoyl-ACP		1.7	1.7	0.53	0.53	$K_{inactivate} = 0.1 \text{ s}^{-1}$
		β -hydroxypalmitoyl-ACP		1.7	1.7	0.53	0.53	$K_3 = 31.2 \text{ s}^{-1}$
		<i>trans</i> -2-deceoyl-ACP	<i>trans</i> -10	1.0×10^{-4}	0.5 ^e	1.65	11.75	$K_{-4} = 90 \text{ s}^{-1}$
								$K_{-5} = 90 \text{ s}^{-1}$
								$K_{degrade} = 5.556 \times 10^{-4} \text{ s}^{-1}$
FabI	12,500 ^a	<i>trans</i> -2-deceoyl-ACP		0.01		20.6		$K_i = 0.035 \text{ Mm}$
		<i>trans</i> -2-dodeceoyl-ACP	<i>trans</i> -12	0.0033 ^h		15 ^h		
		<i>trans</i> -2-tetradecoyl-ACP	<i>trans</i> -14	0.0033		15		
		<i>trans</i> -2-hexadecoyl-ACP	<i>trans</i> -16	0.0033		15		
		<i>trans</i> -3- <i>cis</i> -5-dodeceoyl-ACP	<i>trans</i> -12:1	0.0033		15		
		<i>trans</i> -3- <i>cis</i> -7-tetradecoyl-ACP	<i>trans</i> -14:1	0.0033		15		
		<i>trans</i> -3- <i>cis</i> -9-hexadecoyl-ACP	<i>trans</i> -16:1	0.0033		15		
		(2- <i>trans</i> -11- <i>cis</i>)-vaccen-2-enoyl-ACP	<i>trans</i> -18:1	0.0033		15		
FadR	295 ^a							$K_2 = 0.054 \text{ s}^{-1}$
								$K_{-2} = 0.1 \text{ s}^{-1}$
FabR	295							
PlsB	1,400 ^b	Palmitoyl-ACP	C16	0.015 ^b		13.2		K_{m2} for G3P substrate is
		<i>cis</i> -vaccenoyl-ACP	C18:1	0.025 ^b		11.76		0.14 mM estimated from (b)
PlsC	4,200	Palmitoleoyl-ACP	C16:1	0.012		4.4		K_{m2} for G3P substrate is

	<i>cis</i> -vaccenoyl-ACP	0.025	7.6	0.7 mM estimated from (f)
LpxK				$k = 0.0064 \text{ s}^{-1}$ $k_a = 0.0094 \text{ s}^{-1}$ $K_{inact} = 0.0034 \text{ s}^{-1}$
(a) (45) (b) (46) (c) (54) (d) (55) (e) (15) (f) (39) (g) (11), (h) (59). Parameters that do not have citations are discussed in the main text				

EXPERIMENTAL PROCEDURES

Bacterial strains and growth conditions

The *E. coli* strains and plasmids used in our experiments along with their relevant characteristics are presented in Table S2. Unless stated otherwise, cells were grown in LB medium (10 g tryptone, 5 g yeast extract, 5 g NaCl per litre). When required, antibiotics were used at the following concentrations; 20 µg/ml chloramphenicol, 30 µg/ml kanamycin and 100 µg/ml ampicillin. Protein expression was induced with either L-arabinose or IPTG as appropriate when required.

Table S2: *E. coli* strains and plasmids used in this study and their relevant characteristics

Strains	Relevant characteristics*	Reference
W3110 (wild-type)	λ^- , <i>IN(rrnD-rrnE)1</i> , <i>rph-1</i>	(69)
JP1111	<i>galE45</i> (GalS), λ^- , <i>fabI392</i> (ts), <i>relA1</i> , <i>spoT1</i> , <i>thiE1</i>	(70)
CY53	λ^- , <i>fabA2</i> (ts), <i>relA1</i> , <i>rpsL118</i> (strR), <i>malT1</i> (λ^R), <i>xyl-7</i> , <i>mtlA2</i> , <i>thiE1</i>	(71)
CY288	<i>fhuA22</i> , <i>fabF200</i> , <i>zcf229::Tn10</i> , <i>gyrA220</i> (NalR), <i>fabB15</i> (ts), <i>relA1</i> , <i>rp sL146</i> (strR), <i>pitA10</i> , <i>spoT1</i> , <i>T2R</i>	(54)
Δ FtsH	W3110 <i>zad220::Tn10 sfhC21</i> Δ <i>ftsH3::kan</i>	(72)
DC170	F ⁻ , <i>fabA203</i> (p), <i>fadR16</i> , <i>tyrT58</i> (AS), <i>mel-1</i>	(16)
Plasmids		
pCA24N- <i>waaA</i>	<i>lacI_q</i> , T- <i>rrnB</i> , <i>cat</i> , <i>waaA</i>	(73)
pBO110	P _{BAD} , <i>araC</i> , <i>rrnBT</i> , Amp ^r , <i>lpxC</i>	(32)

* Gene mutations highlighted in bold represent genes involved in fatty acid production/regulation. *sfhC* is a synonym for *fabZ*. The mutation *fabA203*(p) leads to the creation of a novel *fabA* promoter.

Growth conditions for fatty acid biosynthetic mutants

Strain JP1111 (*fabI* (ts)) cells were grown at 30°C to an OD₆₀₀ of 0.15. Part of the culture was transferred to 42°C and grown for 150 min. Growth ceased after 2 generations at the non-permissive temperature. Strain CY288 (*fabB200*, *fabB* (ts)) was prepared as above except that cells were grown in a modified LB broth (5 g tryptone, 2.5 g yeast extract, 2.5 g NaCl) and growth ceased after 2 generations at 42°C. Overnight culture of strain CY53 (*fabA*(ts)) was grown directly either at 30°C or 42°C. At the latter temperature, growth ceased after 3 generations.

Preparation of cell extracts

In the case of the temperature-sensitive mutants, isogenic strains were harvested and re-suspended in TE buffer (10 mM Tris-HCl pH 8.0, 1 mM EDTA) containing 1 mM of Phenylmethylsulfonyl fluoride (PMSF). The cells were lysed by sonication, centrifuged at maximum speed using a microcentrifuge for 1 min, and the protein concentration in the supernatant was determined by the Bradford assay using bovine serum albumin (BSA) as standard (74). 1x Laemmli sample buffer was added to the supernatant and heated at 99°C for 5 min prior to Western blot analysis.

Unless specified otherwise, cell extracts for other strains were prepared as described previously (34, 75). Briefly, an overnight culture was inoculated into fresh LB grown to mid-log phase (OD₆₀₀ = 0.5). The respective cultures were normalized to the same OD₆₀₀ of 0.5. 3 ml of normalized culture was centrifuged at maximum speed for 1 min and the cell pellets re-suspended in 100 µl of TE buffer containing 1x Laemmli sample buffer (Bio-Rad). The samples were heated for 10 min prior to centrifugation for 5 min. The supernatants were collected for Western blot analysis.

Cell extract preparation for in vitro and in vivo LpxC analyses

Both *ftsH* knockout mutant and W3110 strain (wild-type) containing a plasmid bearing the *lpxC* gene were grown at 30°C. 0.1% L-arabinose was included in the growth medium of the latter to induce protein expression. Cells were harvested at mid-log phase, re-suspended in Tris-HCl pH 8.0 (without EDTA) and lysed via sonication. The lysates were added to tubes containing various concentrations of fatty acids and incubated for 10 min at 30°C. When

required, EDTA or PMSF was included in the tubes to inhibit metalloproteases and serine proteases respectively. Sample buffer was added immediately after incubation and heated for 5 min prior to Western blot analysis.

In the assay used to determine the effects of palmitoyl-ACP and palmitoyl-CoA concentrations on LpxC stability *in vivo*, *E. coli* W3110 and *ftsH* knockout mutant cells were grown in LB broth at 30°C to an OD₆₀₀ of 0.1. The cultures were split, CHIR-090 or palmitic acid was added and incubation continued until the OD₆₀₀ reached 0.5. The cultures were normalized according to their density prior to cell extract preparation. Additionally, the *in vivo* LpxC half-life in *ftsH* knockout cells was monitored by initially growing the cells to an OD₆₀₀ of 0.5 after which the cultures were split into different tubes. Specific antibiotics targeting cell wall or membrane synthesis were added for 5 min prior to the addition of 200 µg/ml of chloramphenicol to block protein expression. After 30 min, the cells were shock-frozen in liquid nitrogen and thereafter allowed to thaw on ice prior to cell extract preparation.

Cell extract preparation for WaaA analysis

E. coli wild-type (W3110) cells containing a plasmid bearing the *waaA* gene were grown at 37°C to an OD₆₀₀ of 0.1. Sub-MIC concentration (1/2 MIC) of CHIR-090 was added to part of the culture for 30 min prior to the addition of 0.1 mM IPTG required for protein expression. Growth was allowed to continue for 45 min and the cultures were normalized according to their density prior to harvesting.

Western blot

20 µl of each normalized sample were loaded onto a 10% SDS-polyacrylamide gel. For samples subjected to the Bradford assay, equal amounts of protein were loaded onto each well. Following electrophoresis, proteins were transferred to a PVDF membrane using the Bio-Rad Trans-Blot Turbo system. An LpxC antiserum generated in rabbit (a kind gift from Prof. Franz Narberhaus) and a secondary anti-rabbit peroxidase-linked antibody (Sigma, UK) were used for immunodetection at dilutions of 1:20000 and 1:10000 respectively. The WaaA construct expressed from the plasmid contains a His-tag attached to its N-terminus. Consequently, WaaA was immunoblotted using a 6x-His epitope tag primary antibody

(Pierce) generated in mouse (1:6000) and a secondary anti-mouse alkaline phosphatase-linked (AP) antibody (1:8000). Blots were developed using the ECL chemiluminiscent reagents (Bio-Rad) or AP substrate kit (Bio-Rad) as appropriate. Signals were detected using the ChemiDoc MP system (Bio-Rad). Bands were quantified using the ImageJ software.

LPS quantification

Heptose assay

Heptose levels in LPS were determined by the method described previously (76). Bacterial cultures were normalized prior to harvesting and washed with PBS. LPS was extracted from the membrane according to the method described by Henderson *et al.* (77) and then placed in an ice water bath. 1.125 ml of H₂SO₄ (6 vol. of conc. H₂SO₄ and 1 vol. of H₂O) was added, mixed vigorously, and left in the ice water bath for 3 min. Next, the tubes were transferred to a 25°C water bath for 3 min prior to the addition of 25 µl of 3% cysteine-HCl. The mixture was heated at 99°C for 20 min and absorbance readings were taken after 1 h at 505 nm and 545 nm. The difference in absorbance readings (A₅₀₅ – A₅₄₅) were used for quantitative analyses. The blank was treated as above but with the exclusion of cysteine-HCl.

Kdo assay

LPS was also quantified by measuring the concentration of 3-deoxy-D-manno-oct-2-ulosonic (Kdo) in either membrane fractions, or extracted LPS according to the method described by Karkhanis *et al* (78). For Kdo analysis on membrane fractions, harvested cells were washed with PBS and re-suspended in TE buffer containing 1 mg/ml lysozyme. Cells were further sonicated and centrifuged for 20 min at 13,000 rpm. The membrane fraction were subsequently analyzed.

In order to determine the amount (in nmoles) of heptose and Kdo sugars, LPS was extracted from a 3 ml normalized culture harvested at an OD₆₀₀ of 0.5. The weight (in µg) of both sugars from the extracted LPS were derived from standard curves presented previously (76, 78). With knowledge of the molecular weight of heptose and Kdo sugars (210.18 and 238.19 g/mol respectively), the amounts were calculated.

Phenotypic characterization on agar plates

E. coli strains containing the plasmid bearing the *waaA* gene were grown to an OD₆₀₀ of 0.2 and serial dilutions from 10⁻¹ to 10⁻⁴ were prepared. 2 µl of the dilutions were spotted on LB agar plates containing chloramphenicol and when required, IPTG was used to induce expression. The plates were incubated at 30°C overnight.

Fatty acid analysis

Fatty acid extraction

Fatty acid extraction was performed essentially as described by Kurkiewicz *et al* (79). 40 ml of normalized bacteria cells harvested at an OD₆₀₀ of approximately 0.5 were centrifuged and the pellets heated with 3M NaOH (1 ml) for 40 min at 90°C in a water bath. 2ml of 3.25M HCl was added and heated further for 10 min at the same temperature. After cooling, fatty acids were extracted 3 times using 1ml of hexane-diethyl ether mixture (1:1). The organic layers were separated by centrifugation for 5 min at 2400 x g. The obtained fatty acids were evaporated under vacuum prior to the derivatization step.

Preparation of 3-pyridylcarbinol (picolinyl) ester derivatives

The derivatives were prepared as described previously (80). The extracted fatty acids were heated with 20 µl of thionyl chloride for 10 min at 99°C. The residual thionyl chloride was evaporated under a stream of nitrogen gas and a solution of 20% 3-(hydroxymethyl) pyridine in acetonitrile (10 µl) was added. The mixture was heated for 1 min at 99°C. 500 µl of hexane was added prior to GCMS analysis.

Gas chromatography-mass spectrometry

GCMS analyses were performed using an Agilent GC 7890A and EI/CI MSD 5975C models. Chromatographic separations were performed using a capillary column (30 m, 0.25 mm i.d., 0.25 µm film thickness) and helium was the carrier gas. The temperature program of the oven used were those previously described by Oursel *et al.* (64); initial temperature at 200°C, held for 1 min, raised to 240°C at 8°C min⁻¹, then ramped to 300°C at 2°C min⁻¹.

Peak identities were confirmed from their electron ionization (EI) mass spectra, and comparison with retention times of known standards.

SUPPLEMENTARY RESULTS

Overexpression of *fabA* enhances LpxC degradation

When strain DC170 (*fabAup*) which overexpresses *fabA* was grown at 30°C, there were no differences in LpxC levels relative to the control strain (W3110). However, at 42°C, we observed a rapid degradation of LpxC (Fig. S4A). Clark *et al.* (16) had reported previously that saturated fatty acid levels are not elevated in strains overexpressing *fabA* at temperatures of 30°C or less; however, at optimum temperature and especially 42°C, saturated fatty acids concentration were significantly increased. As we have stipulated in the main article text, excess flux of substrates into the saturated fatty acid pathway and subsequently the LPS pathway enhances LpxC degradation which most likely explains the results presented in Fig. S4A. Furthermore, we observed that the amount of LPS synthesized at both temperatures by strain DC170 were similar to those of wild-type (Fig. S4B). In particular, at 42°C in which pathway substrate flux was increased, an increment in LPS relative to wild-type is not expected because LpxK becomes the rate-limiting step. Instead, lipid A disaccharide would accumulate leading to a rapid degradation of LpxC (Fig. S4A).

We also observed that overexpression of *lpxC* was highly toxic in strain DC170 and under such condition, cells spend a significant length of time in the lag growth phase presumably to degrade excess LpxC prior to reproduction (Fig. S4C). This also supports the claim that LpxC level must be lowered under *fabA* overexpression conditions.

Overexpression of *waaA* is toxic to cells

When we overexpressed *waaA*, cell growth was inhibited (Fig. S5B). A similar finding was observed previously for LpxC in studies by Fuhrer *et al.* in which overexpression of a functional *lpxC* gene resulted in cell toxicity (32). The authors also observed that overexpression of non-functional *lpxC* did not result in cell toxicity. Therefore, it is plausible that under unregulated WaaA conditions, such as during overexpression, increased metabolic activity occurs which is undesirable to the cell. Additionally, when we reduced the LPS pathway flux by inhibiting LpxC using sub-MIC concentration of CHIR-090, overexpression of *waaA* under this condition did not prevent cellular toxicity (Fig. S5C). This provided an indication that unregulated production of WaaA would also result in increased metabolic

activity which may be independent on LPS production rate. In fact, the toxicity induced by *waaA* overexpression and LpxC inhibition was additive (Fig. S5C).

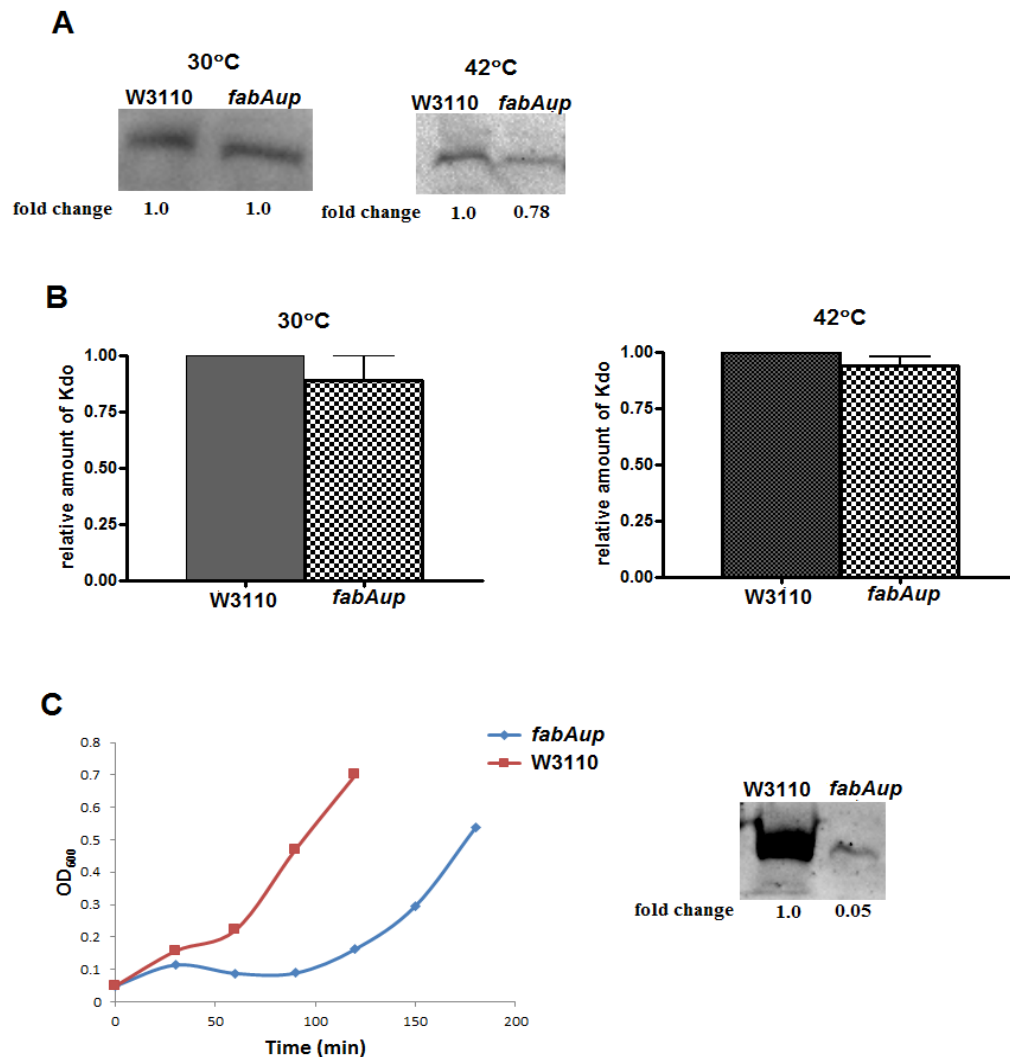


Fig. S4. Effect of *fabA* overexpression on LPS regulation. (A) LpxC levels in W3110 and DC170 (*fabAup*). (B) LPS quantification in both W3110 and DC170 strains. LPS was quantified by measuring the amount of Kdo in the membrane. (C) Strains W3110 and DC170 were transformed with a plasmid bearing the *lpxC* gene (pBO110) and protein expression was induced overnight at 30°C using 0.1% L-arabinose. Overnight cells were transferred to fresh broth (without inducer) and incubated at 42°C. Growth rate was monitored (left) and after 90 min, part of the culture was harvested, and cell extracts subjected to the Bradford assay prior to Western blot analysis (right).

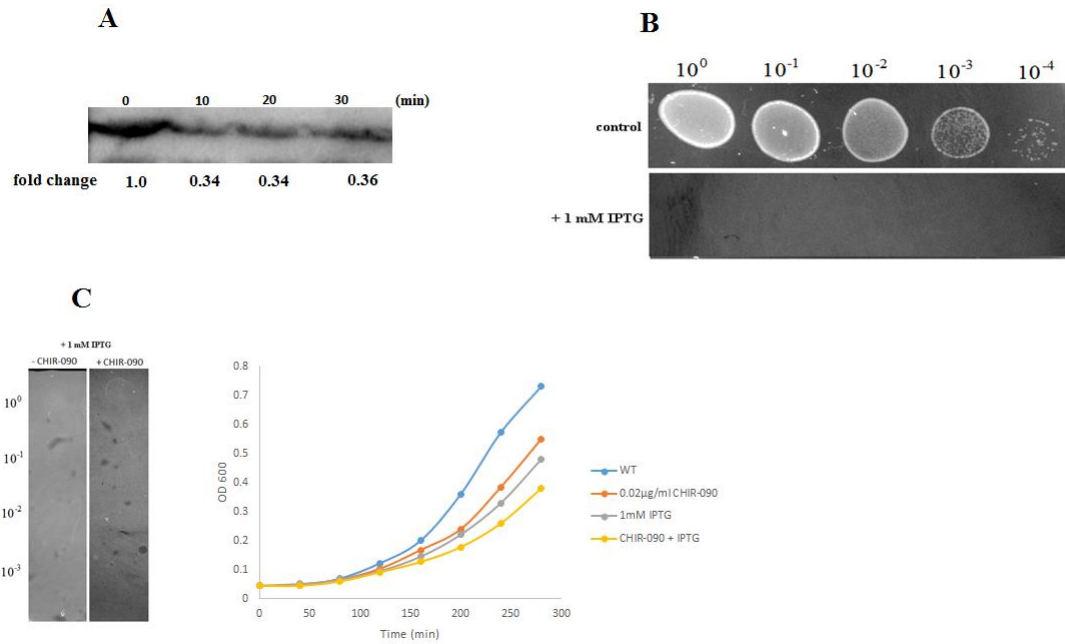


Fig. S5. *waaA* overexpression. (A) *E. coli* (W3110) strain was transformed with a plasmid bearing the *waaA* gene which had histidine (6x-His) tagged to its N-terminus region. Because gene fusions either to the N- or C- terminus region can prevent the proteolytic regulation of its protein product (32, 81), it was crucial to ensure that the *waaA* plasmid construct was suitable for experimental investigations. In this regard, the WaaA half-life was monitored by inducing protein expression using IPTG. Cells were grown at 37°C in LB broth with the addition of 20 μg/ml of chloramphenicol. At an OD₆₀₀ of 0.5, *waaA* expression was induced using 0.1 mM of IPTG for 10 min prior to the addition of 300 μg/ml of spectinomycin to block protein translation. 3 ml of culture were dispensed in various Eppendorf tubes and were shock frozen in liquid nitrogen to stop all cellular processes. The indicated time points represent min after the addition of spectinomycin in which cells were frozen. The cells were allowed to thaw on ice and harvested prior to Western blot analysis. A half-life of approximately 7 min was obtained which is in agreement with prior observations for chromosomally expressed WaaA (43). (B) Overexpression of *waaA* is toxic to cells. Cells were grown on LB agar plates. (C) Cell growth was severely inhibited under LPS pathway flux inhibition with CHIR-090 (left). The concentration of CHIR-090 utilized was 0.02 μg/ml. The combined toxicity resulting from *waaA* overexpression and CHIR-090 treatment is additive (right).

Table S3: MIC of different antibiotics under *waaA* overexpression.

	Uninduced	0.1 mM IPTG induction	1 mM IPTG induction
Colistin ($\mu\text{g/ml}$)	1	0.5	0.25
Bacitracin (mg/ml)	5	5	5
Vancomycin (mg/ml)	0.5	0.5	0.0625
Triton X-100 (%)	>20	>20	20
SDS (%)	0.156	0.156	0.078
Erythromycin (mg/ml)	0.125	0.125	0.0625
Kanamycin ($\mu\text{g/ml}$)	8	8	1

E. coli wild-type (W3110) cells containing a plasmid bearing the *waaA* gene were grown at 37°C to an OD₆₀₀ of 0.1 prior to addition of IPTG to induce expression. Growth was allowed to continue for 2 h and the cultures were normalized according to their density prior to harvesting.

SUPPLEMENTARY REFERENCES

1. Heath, RJ, Jackowski, S, Rock, CO (2002) Fatty acid and phospholipid metabolism in prokaryotes. *Biochemistry of Lipids, Lipoproteins, and Membranes*, eds Vance DE, Vance JE (Elsevier Science Publishing Co., New York), pp. 55-92.
2. Janßen, HJ, Steinbüchel, A (2014) Fatty acid synthesis in *Escherichia coli* and its applications towards the production of fatty acid based biofuels. *Biotechnol Biofuels* 7(1): 7. doi: 10.1186/1754-6834-7-7.
3. Cronan, JE, Waldrop, GL (2002) Multi-subunit acetyl-CoA carboxylases. *Prog Lipid Res* 41(5): 407-435.
4. Choi-Rhee, E, Cronan, JE (2003) The biotin carboxylase-biotin carboxyl carrier protein complex of *Escherichia coli* acetyl-CoA carboxylase. *J Biol Chem* 278(33): 30806-30812. doi: 10.1074/jbc.M302507200.
5. Li, SJ, Cronan, JE (1993) Growth rate regulation of *Escherichia coli* acetyl coenzyme A carboxylase, which catalyses the first committed step of lipid biosynthesis. *J Bacteriol* 175(2): 332-340.
6. James, ES, Cronan, JE (2004) Expression of two *Escherichia coli* acetyl-CoA carboxylase subunits is autoregulated. *J Biol Chem* 279(4): 2520-2527. doi: 10.1074/jbc.M311584200.
7. Davis, MS, Cronan, JE (2001) Inhibition of *Escherichia coli* acetyl coenzyme A carboxylase by acyl-acyl carrier protein. *J Bacteriol* 183(4): 1499-1503. doi: 10.1128/JB.183.4.1499-1503.2001.
8. Zhang, Y, Cronan, JE (1998) Transcriptional analysis of essential genes of the *Escherichia coli* fatty acid biosynthesis gene cluster by functional replacement with the analogous *Salmonella typhimurium* gene cluster. *J Bacteriol* 180(13): 3295-3303.
9. Magnuson, K, Oh, W, Larson, TJ, Cronan, JE (1992) Cloning and nucleotide sequence of the *fabD* gene encoding malonyl coenzyme A-acyl carrier protein transacylase of *Escherichia coli*. *FEBS Lett* 299(3): 262-266.
10. Garwin, JL, Klages, AL, Cronan, JE (1980) Beta-ketoacyl-acyl carrier protein synthase II of *Escherichia coli*. Evidence for function in the thermal regulation of fatty acid synthesis. *J Biol Chem* 255(8): 3263-3265.
11. Heath, RJ, Rock, CO (1996) Inhibition of beta-ketoacyl-acyl carrier protein synthase III (*FabH*) by acyl-acyl carrier protein in *Escherichia coli*. *J Biol Chem* 271(18): 10996-11000.
12. Toomey, RE, Wakil, SJ (1966) Studies on the mechanism of fatty acid synthesis. Preparation and general properties of beta-ketoacyl acyl carrier protein reductase from *Escherichia coli*. *Biochim Biophys Acta* 116(2): 189-197.
13. Heath, RJ, Rock, CO (1996) Roles of the *FabA* and *FabZ* beta-hydroxyacyl-acyl carrier protein dehydratases in *Escherichia coli* fatty acid biosynthesis. *J Biol Chem*, 271(44): 27795-27801.
14. Heath, RJ, Rock, CO (1995) Enoyl-acyl carrier protein reductase (*fabI*) plays a determinant role in completing cycles of fatty acid elongation in *Escherichia coli*. *J Biol Chem* 270(44): 26538-26542.
15. Kass, LR, Brock, DJ, Bloch, K (1967) Beta-hydroxydecanoyl thioester dehydrase. I. Purification and properties. *J Biol Chem* 242(19): 4418-4431.

16. Clark, DP, DeMendoza, D, Polacco, ML, Cronan, JE (1983) Beta-hydroxydecanoyl thio ester dehydrase does not catalyse a rate-limiting step in Escherichia coli unsaturated fatty acid synthesis. *Biochemistry* 22(25): 5897-5902.
17. Cao, Y, Yang, J, Xian, M, Xu, X, Liu, W (2010) Increasing unsaturated fatty acid contents in Escherichia coli by coexpression of three different genes. *Appl Microbiol Biotechnol* 87(1): 271-280. doi: 10.1007/s00253-009-2377-x.
18. Edwards, P, Nelsen, JS, Metz, JG, Dehesh, K (1997) Cloning of the fabF gene in an expression vector and in vitro characterization of recombinant fabF and fabB encoded enzymes from Escherichia coli. *FEBS Lett* 402(1): 62-66.
19. Cronan, JE, Birge, CH, Vagelos, PR (1969) Evidence for two genes specifically involved in unsaturated fatty acid biosynthesis in Escherichia coli. *J Bacteriol* 100(2): 601-604.
20. Subrahmanyam, S, Cronan, JE (1998) Overproduction of a functional fatty acid biosynthetic enzyme blocks fatty acid synthesis in Escherichia coli. *J Bacteriol* 180(17): 4596-4602.
21. Nunn, WD, Giffin, K, Clark, D, Cronan, JE (1983) Role for fadR in unsaturated fatty acid biosynthesis in Escherichia coli. *J Bacteriol* 154(2): 554-560.
22. Zhang, YM, Marrakchi, H, Rock, CO (2002) The FabR (YijC) transcription factor regulates unsaturated fatty acid biosynthesis in Escherichia coli. *J Biol Chem* 277(18): 15558-15565. doi: 10.1074/jbc.M201399200.
23. Feng, Y, Cronan, JE (2012) Crosstalk of Escherichia coli FadR with global regulators in expression of fatty acid transport genes. *PLoS One* 7(9): e46275. doi: 10.1371/journal.pone.0046275.
24. Feng, Y, Cronan, JE (2009) Escherichia coli unsaturated fatty acid synthesis: complex transcription of the fabA gene and in vivo identification of the essential reaction catalysed by FabB. *J Biol Chem* 284(43): 29526-29535. doi: 10.1074/jbc.M109.023440.
25. Feng, Y, Cronan, JE (2011) Complex binding of the FabR repressor of bacterial unsaturated fatty acid biosynthesis to its cognate promoters. *Mol Microbiol* 80(1): 195-218. doi: 10.1111/j.1365-2958.2011.07564.x.
26. Campbell, JW, Cronan, JE (2001) Escherichia coli FadR positively regulates transcription of the fabB fatty acid biosynthetic gene. *J Bacteriol* 183(20): 5982-5990. doi: 10.1128/JB.183.20.5982-5990.2001.
27. Zhu, K, Zhang, YM, Rock, CO (2009) Transcriptional regulation of membrane lipid homeostasis in Escherichia coli. *J Biol Chem* 284(50): 34880-34888. doi: 10.1074/jbc.M109.068239.
28. Simons, RW, Egan, PA, Chute, HT, Nunn, WD (1980) Regulation of fatty acid degradation in Escherichia coli: isolation and characterization of strains bearing insertion and temperature-sensitive mutations in gene fadR. *J Bacteriol* 142(2): 621-632.
29. Lai, CY, Cronan, JE (2004) Isolation and characterization of beta-ketoacyl-acyl carrier protein reductase (fabG) mutants of Escherichia coli and Salmonella enterica serovar Typhimurium. *J Bacteriol* 186(6): 1869-1878.
30. Ogura, T et al. (1999) Balanced biosynthesis of major membrane components through regulated degradation of the committed enzyme of lipid A biosynthesis by the AAA protease FtsH (HflB) in Escherichia coli. *Mol Microbiol* 31(3): 833-844.

31. Schäkermann, M, Langklotz, S, Narberhaus, F (2013) FtsH-Mediated Coordination of Lipopolysaccharide Biosynthesis in Escherichia coli Correlates with the Growth Rate and the Alarmone (p)ppGpp. *J Bacteriol* 195(9): 1912-1919. doi: 10.1128/JB.02134-12.
32. Führer, F, Langklotz, S, Narberhaus, F (2006) The C-terminal end of LpxC is required for degradation by the FtsH protease. *Mol Microbiol* 59(3): 1025-1036. doi: 10.1111/j.1365-2958.2005.04994.x.
33. Emiola, A, George, J, Andrews, SS (2014) A Complete Pathway Model for Lipid A Biosynthesis in Escherichia coli. *PLoS One* 10(4): e0121216. doi: 10.1371/journal.pone.0121216.
34. Zeng, D et al. (2013) Mutants resistant to LpxC inhibitors by rebalancing cellular homeostasis. *J Biol Chem* 288(8): 5475-5486. doi: 10.1074/jbc.M112.447607.
35. Heath, RJ, Rock, CO (1996) Regulation of fatty acid elongation and initiation by acyl-acyl carrier protein in Escherichia coli. *J Biol Chem* 271(4): 1833-1836.
36. Egan, AF, Russell, RR (1973) Conditional mutations affecting the cell envelope of Escherichia coli K-12. *Genet Res* 21(2): 139-152.
37. Xu, HH, Real, L, Bailey, MW (2006) An array of Escherichia coli clones over-expressing essential proteins: a new strategy of identifying cellular targets of potent antibacterial compounds. *Biochem Biophys Res Commun* 349(4): 1250-1257. doi: 10.1016/j.bbrc.2006.08.166.
38. Goelz, SE, Cronan, JE (1980) The positional distribution of fatty acids in Escherichia coli phospholipids is not regulated by sn-glycerol 3-phosphate levels. *J Bacteriol* 144(1): 462-464.
39. Rock, CO, Goelz, SE, Cronan, JE (1981) Phospholipid synthesis in Escherichia coli. Characteristics of fatty acid transfer from acyl-acyl carrier protein to sn-glycerol 3-phosphate. *J Biol Chem* 256(2): 736-742.
40. Raetz, CR (1978) Enzymology, genetics, and regulation of membrane phospholipid synthesis in Escherichia coli. *Microbiol Rev* 42(3): 614-659.
41. Raetz, CR et al. (2009) Discovery of new biosynthetic pathways: the lipid A story. *J Lipid Res*, 50 Suppl: S103-108. doi: 10.1194/jlr.R800060-JLR200.
42. Anderson, MS et al. (1993) UDP-N-acetylglucosamine acyltransferase of Escherichia coli. The first step of endotoxin biosynthesis is thermodynamically unfavourable. *J Biol Chem* 268(26): 19858-19865.
43. Katz, C, Ron, EZ (2008) Dual role of FtsH in regulating lipopolysaccharide biosynthesis in Escherichia coli. *J Bacteriol* 190(21): 7117-7122. doi: 10.1128/JB.00871-08.
44. Ray, BL, Raetz, CR (1987) The biosynthesis of gram-negative endotoxin. A novel kinase in Escherichia coli membranes that incorporates the 4'-phosphate of lipid A. *J Biol Chem* 262(3): 1122-1128.
45. Ishihama, Y et al (2008) Protein abundance profiling of the Escherichia coli cytosol. *BMC Genomics*, 9: 102. doi: 10.1186/1471-2164-9-102.
46. Green, PR, Merrill, AH, Bell, RM. (1981) Membrane phospholipid synthesis in Escherichia coli. Purification, reconstitution, and characterization of sn-glycerol-3-phosphate acyltransferase. *J Biol Chem* 256(21): 11151-11159.

47. Jiang, P, Cronan, JE (1994) Inhibition of fatty acid synthesis in *Escherichia coli* in the absence of phospholipid synthesis and release of inhibition by thioesterase action. *J Bacteriol* 176(10): 2814-2821.
48. Bergler, H, Fuchsbichler, S, Högenauer, G, Turnowsky, F (1996) The enoyl-[acyl-carrier-protein] reductase (FabI) of *Escherichia coli*, which catalyses a key regulatory step in fatty acid biosynthesis, accepts NADH and NADPH as cofactors and is inhibited by palmitoyl-CoA. *Eur J Biochem* 242(3): 689-694.
49. Cornish-Bowden, A, Cárdenas, ML (2001) Information transfer in metabolic pathways. Effects of irreversible steps in computer models. *Eur J Biochem* 268(24): 6616-6624.
50. Mendes, P, Hoops, S, Sahle, S, Gauges, R, Dada, J, Kummer, U (2009) Computational modeling of biochemical networks using COPASI. *Methods Mol Biol* 500: 17-59. doi: 10.1007/978-1-59745-525-1_2.
51. Zhang, YM, Wu, B, Zheng, J, Rock, CO (2003) Key residues responsible for acyl carrier protein and beta-ketoacyl-acyl carrier protein reductase (FabG) interaction. *J Biol Chem* 278(52): 52935-52943. doi: 10.1074/jbc.M309874200.
52. Sun, YH, Cheng, Q, Tian, WX, Wu, XD (2008) A substitutive substrate for measurements of beta-ketoacyl reductases in two fatty acid synthase systems. *J Biochem Biophys Methods* 70(6): 850-856. doi: 10.1016/j.jbbm.2007.10.005.
53. Wilks, JC, Slonczewski, JL (2007) pH of the cytoplasm and periplasm of *Escherichia coli*: rapid measurement by green fluorescent protein fluorimetry. *J Bacteriol* 189(15): 5601-5607. doi: 10.1128/JB.00615-07.
54. Garwin, JL, Klages, AL, Cronan, JE (1980) Structural, enzymatic, and genetic studies of beta-ketoacyl-acyl carrier protein synthases I and II of *Escherichia coli*. *J Biol Chem* 255(24): 11949-11956.
55. D'Agnolo, G, Rosenfeld, IS, Vagelos, PR (1975) Multiple forms of beta-ketoacyl-acyl carrier protein synthetase in *Escherichia coli*. *J Biol Chem* 250(14): 5289-5294.
56. Helmkamp, GM, Brock, DJ, Bloch, K (1968) Beta-hydroxydecanolyl thioester dehydrase. Specificity of substrates and acetylenic inhibitors. *J Biol Chem* 243(12): 3229-3231.
57. Coleman, J (1992) Characterization of the *Escherichia coli* gene for 1-acyl-sn-glycerol-3-phosphate acyltransferase (plsC). *Mol Gen Genet* 232(2): 295-303.
58. Weeks, G, Wakil, SJ (1968) Studies on the mechanism of fatty acid synthesis. Preparation and general properties of the enoyl acyl carrier protein reductases from *Escherichia coli*. *J Biol Chem* 243(6): 1180-1189.
59. Rafi, SB et al. (2006) Insight through molecular mechanics Poisson-Boltzmann surface area calculations into the binding affinity of triclosan and three analogues for FabI, the *E. coli* enoyl reductase. *J Med Chem* 49(15): 4574-4580. doi: 10.1021/jm060222t.
60. Yao, Z, Davis, RM, Kishony, R, Kahne, D, Ruiz, N (2012) Regulation of cell size in response to nutrient availability by fatty acid biosynthesis in *Escherichia coli*. *Proc Natl Acad Sci U S A* 109(38): E2561-2568. doi: 10.1073/pnas.1209742109.
61. Galloway, SM, Raetz, CR (1990) A mutant of *Escherichia coli* defective in the first step of endotoxin biosynthesis. *J Biol Chem* 265(11): 6394-6402.
62. Cayley, S, Lewis, BA, Guttman, H.J, Record, MT (1991) Characterization of the cytoplasm of *Escherichia coli* K-12 as a function of external osmolarity. Implications for protein-DNA interactions in vivo. *J Mol Biol* 222(2): 281-300

63. Mackie, GA (2013) RNase E: at the interface of bacterial RNA processing and decay. *Nat Rev Microbiol* 11(1): 45-57. doi: 10.1038/nrmicro2930.
64. Oursel, D et al. (2007) Identification and relative quantification of fatty acids in Escherichia coli membranes by gas chromatography/mass spectrometry. *Rapid Commun Mass Spectrom* 21(20): 3229-3233. doi: 10.1002/rcm.3177.
65. Schlame, M, Brody, S, Hostetler, KY (1993) Mitochondrial cardiolipin in diverse eukaryotes. Comparison of biosynthetic reactions and molecular acyl species. *Eur J Biochem* 212(3): 727-735
66. Onishi, HR et al. (1996) Antibacterial agents that inhibit lipid A biosynthesis. *Science* 274(5289): 980-982.
67. Lee, S, Jung, Y, Lee, J (2013) Correlations between FAS elongation cycle genes expression and fatty acid production for improvement of long-chain fatty acids in Escherichia coli. *Appl Biochem Biotechnol* 169(5): 1606-1619. doi: 10.1007/s12010-012-0088-8.
68. Tsay, JT, Oh, W, Larson, TJ, Jackowski, S, Rock, CO (1992) Isolation and characterization of the beta-ketoacyl-acyl carrier protein synthase III gene (fabH) from Escherichia coli K-12. *J Biol Chem* 267(10): 6807-6814.
69. Bachmann, BJ (1972) Pedigrees of some mutant strains of Escherichia coli K-12. *Bacteriol Rev* 36(4): 525-557.
70. Egan, AF, Russell, RR (1973) Conditional mutations affecting the cell envelope of Escherichia coli K-12. *Genet Res* 21(2): 139-152.
71. Cronan, JE, Silbert, DF, Wulff, DL (1972) Mapping of the fabA locus for unsaturated fatty acid biosynthesis in Escherichia coli. *J Bacteriol* 112(1): 206-211.
72. Tatsuta, T et al. (1998) Heat shock regulation in the ftsH null mutant of Escherichia coli: dissection of stability and activity control mechanisms of sigma32 in vivo. *Mol Microbiol* 30(3): 583-593.
73. Kitagawa, M et al. (2005) Complete set of ORF clones of Escherichia coli ASKA library (a complete set of E. coli K-12 ORF archive): unique resources for biological research. *DNA Res* 12(5): 291-299. doi: 10.1093/dnares/dsi012.
74. Bradford, MM (1976) A rapid and sensitive method for the quantitation of microgram quantities of protein utilizing the principle of protein-dye binding. *Anal Biochem* 72: 248-254.
75. Sorensen, PG et al. (1996) Regulation of UDP-3-O-[R-3-hydroxymyristoyl]-N-acetylglucosamine deacetylase in Escherichia coli. The second enzymatic step of lipid A biosynthesis. *J Biol Chem* 271(42): 25898-25905.
76. Wright, BG, Rebers, PA (1972) Procedure for determining heptose and hexose in lipopolysaccharides. Modification of the cysteine-sulfuric acid method. *Anal Biochem*, 49(2): 307-319.
77. Henderson, JC, O'Brien, JP, Brodbelt, JS, Trent, MS (2013) Isolation and chemical characterization of lipid A from gram-negative bacteria. *J Vis Exp* (79): e50623. doi: 10.3791/50623.
78. Karkhanis, YD, Zeltner, JY, Jackson, JJ, Carlo, DJ (1978) A new and improved microassay to determine 2-keto-3-deoxyoctonate in lipopolysaccharide of Gram-negative bacteria. *Anal Biochem* 85(2): 595-601.
79. Kurkiewicz, S, Dzierzewicz, Z, Wilczok, T, Dworzanski, JP (2003) GC/MS determination of fatty acid picolinyl esters by direct curie-point pyrolysis of whole

- bacterial cells. *J Am Soc Mass Spectrom* 14(1): 58-62. doi: 10.1016/S1044-0305(02)00817-6.
80. Harvey, DJ (1998) Picolinyl esters for the structural determination of fatty acids by GC/MS. *Mol Biotechnol* 10(3): 251-260. doi: 10.1007/BF02740846.
 81. Führer, F et al. (2007) Sequence and length recognition of the C-terminal turnover element of LpxC, a soluble substrate of the membrane-bound FtsH protease. *J Mol Biol*, 372(2): 485-496. doi: 10.1016/j.jmb.2007.06.083.